

# 1 **Automation of soil flux chamber measurements: potentials** 2 **and pitfalls**

3

4 **Carolyn-Monika Görres<sup>1,2</sup>, Claudia Kammann<sup>2</sup>, and Reinhart Ceulemans<sup>1</sup>**

5 [1]{Center of Excellence PLECO (Plant and Vegetation Ecology), University of Antwerp,  
6 Universiteitsplein 1, 2610 Wilrijk, Belgium}

7 [2]{WG Global Change Research in Special Crops, Department of Soil Science and Plant  
8 Nutrition, Hochschule Geisenheim University, Von-Lade-Str. 1, 65366 Geisenheim, Germany}

9 Correspondence to: C.-M. Görres (carolyn.gorres@hs-gm.de)

10

## 11 **Abstract**

12 Recent technological advances have enabled the wider application of automated chambers for  
13 soil greenhouse gas (GHG) flux measurements, several of them commercially available.  
14 However, few studies addressed the challenges associated with operating these systems. In this  
15 contribution we compared two commercial soil GHG chamber systems – the LI-8100A  
16 Automated Soil CO<sub>2</sub> Flux System and the Greenhouse Gas Monitoring System AGPS. From  
17 April 2014 until August 2014, the two systems monitored in parallel soil respiration (SR) fluxes  
18 at a recently harvested poplar (*Populus*) plantation, which provided a bare field situation  
19 directly after the harvest as well as a closed canopy later on. For the bare field situation (15  
20 April – 30 June 2014), the cumulated average SR obtained from the unfiltered datasets of the  
21 LI-8100A and the AGPS were 520 and 433 g CO<sub>2</sub> m<sup>-2</sup>, respectively. For the closed canopy  
22 phase (01 July – 31 August 2014), which was characterized by a higher soil moisture content,  
23 the cumulated average SR estimates were not significantly different with 507 and 501 g CO<sub>2</sub>  
24 m<sup>-2</sup> for the AGPS and the LI-8100A, respectively. Flux quality control and filtering did not  
25 significantly alter the results obtained by the LI-8100A, whereas the AGPS SR estimates were  
26 reduced by at least 20 %. The main reasons for the observed differences in the performance of  
27 the two systems were (i) a lower data coverage provided by the AGPS due to technical  
28 problems; (ii) incomplete headspace mixing in the AGPS chambers; (iii) lateral soil CO<sub>2</sub>  
29 diffusion below the collars during AGPS chamber measurements; and (iv) a possible  
30 overestimation of nighttime SR fluxes by the LI-8100A. Additionally, increased root growth

1 was observed within the LI-8100 collars, but not within the AGPS collars, which might have  
2 also contributed to the observed differences. In contrast to the LI-8100A, the AGPS had the gas  
3 sample inlets installed inside the collars and not the chambers. This unique design feature  
4 enabled for the first time the detection of disturbed chamber measurements during nights with  
5 a stratified atmosphere, resulting in unbiased nighttime SR estimates. Thus besides providing  
6 high temporal frequency flux data, automated chamber systems offer another possibility to  
7 greatly improve our understanding of SR fluxes.

## 8 9 **1 Introduction**

10 The majority of soil greenhouse gas (GHG) flux data has been obtained using manually  
11 operated closed static chambers (Pumpanen et al., 2004; Levy et al., 2011). These chambers are  
12 placed air-tight on a small soil area (typically  $<1 \text{ m}^2$  and  $<1 \text{ h}$ ) and gas samples are collected  
13 from the chambers during the closure time. The gas samples are subsequently analysed by gas  
14 chromatography or other analytical techniques and the flux is calculated from the rate of gas  
15 concentration change over time (Levy et al., 2011; Collier et al., 2014). The chamber design  
16 and measurement protocol are highly flexible and can be adjusted for different ecosystems or  
17 land use types, and this at relatively low costs (Pumpanen et al., 2004; de Klein and Harvey,  
18 2012). A major drawback, however, is the low temporal resolution since working with manual  
19 closed chambers is very laborious, and measurements are thus only performed at low or  
20 irregular frequency (every few days or weeks) (Savage et al., 2014; Koskinen et al., 2014). As  
21 a result, our knowledge of short-term responses of soil GHG flux dynamics to perturbations  
22 such as rain events, irrigation and fertilization, but also of the diurnal cycles of soil GHG fluxes  
23 and associated time lags is still very limited (Carbone and Vargas, 2008; Vargas et al., 2011;  
24 Hopkins et al., 2013; Phillips et al., 2013). One of the key challenges of contemporary GHG  
25 flux research is to close these knowledge gaps in order to improve the quantitative prediction  
26 of GHG fluxes (Giltrap et al., 2010; FAO, 2014; Olander et al., 2014; Savage et al., 2014).

27 One approach to obtain high temporal frequency soil GHG flux data is the automation of  
28 chamber measurements. Automated chambers have been in use since the 1970s (Denmead,  
29 1979) and different systems have been developed over the years (e.g. Breuer et al., 2000;  
30 Ambus et al., 2010; Koskinen et al., 2014; Savage et al., 2014). The total number of studies  
31 with automated chambers remains, however, quite low and the majority of them only deals with  
32 soil  $\text{CO}_2$  fluxes. The latter is mainly due to a lack of available field gas analysers for  $\text{CH}_4$  and

1 N<sub>2</sub>O in the past (Venterea et al., 2008; Savage et al., 2014). The requirements for a larger  
2 infrastructure and for intensive maintenance as compared to manual chamber measurements  
3 have prevented the widespread application of automated systems. Therefore, only a few studies  
4 actually address the difficulties and challenges associated with running these systems  
5 (Koskinen et al., 2014).

6 In general chambers provide an invasive method and, depending on the design, they alter soil  
7 and microclimatic conditions to a degree that can potentially bias the measured fluxes. Potential  
8 biases introduced by different chamber designs and sampling procedures have been quantified  
9 in numerous studies (Pumpanen et al., 2004; Christiansen et al., 2011; Pihlatie et al., 2013;  
10 Görres et al., 2014), and the elimination of these biases is an ongoing debate (de Klein and  
11 Harvey, 2012). Several studies have compared the data quality of automated chamber systems  
12 with manually operated chambers (Savage et al., 2014), with soil gas concentration profile  
13 measurements (Jassal et al., 2005; Roland et al., 2015) and with the eddy covariance method  
14 (Wang et al., 2013). However, different automated chamber systems have never been compared  
15 in the field as has been done for eddy covariance flux systems (Janssens et al., 2000; Peltola et  
16 al., 2013).

17 Due to technological advances, more automated chamber systems are commercially available,  
18 and an increasing number of custom-made systems are being designed and deployed for soil  
19 GHG flux measurements (de Klein and Harvey, 2012). Comparative analyses are important to  
20 guarantee high quality data collection with these systems and a high comparability among  
21 studies using different systems (Janssens et al., 2000; Creelman et al., 2013). Here we present  
22 a detailed field comparison of two automated soil GHG flux systems – the LI-8100A Soil CO<sub>2</sub>  
23 Flux System and the Automated Gas Sampling System AGPS. The LI-8100A is a fully  
24 automated chamber system including multiplexer, gas analyser and flux calculation software.  
25 The AGPS is a commercially available automated vial collector system in which each  
26 automated chamber operates as an autonomous unit and the collected gas samples have to be  
27 subsequently analysed by gas chromatography (Kitzler et al., 2006). For this study, the AGPS  
28 has been equipped with a multiplexer and gas analysers for the first time, resembling a fully  
29 automated custom-made chamber system with continuous gas analysis in the field. In parallel,  
30 both systems were monitoring soil respiration (SR) in a coppiced poplar plantation. The poplar  
31 plantation had the advantage that it provided open field conditions as well as closed canopy  
32 conditions within one vegetation period. In addition to the chamber measurements, CO<sub>2</sub>

1 concentrations were monitored in the topsoil to give insights into the potential range of soil CO<sub>2</sub>  
2 fluxes at the site and to better understand the performance of the chambers under different soil  
3 moisture conditions. The aim of this study was not to understand the processes driving SR or  
4 soil CO<sub>2</sub> efflux at the poplar plantation per se since these have already been discussed amongst  
5 others by Verlinden et al. (2013) and Zenone et al. (2015). The results presented here serve the  
6 comparison of the performance of the two chamber systems in quantifying SR fluxes under a  
7 wide range of different environmental conditions.

## 8 9 **2 Materials and Methods**

### 10 **2.1 Field site and experimental design**

11 This study was conducted in a short-rotation poplar (*Populus*) bioenergy plantation located in  
12 Flanders, Belgium (51°06'44'' N, 3°51'02'' E). The plantation had been established in spring  
13 2010 in a double-row planting system, i.e. the distance between two adjacent rows of poplar  
14 trees alternated between 0.75 m and 1.50 m (hereafter referred to as narrow and wide rows,  
15 respectively). Within a row, the poplars were planted 1.10 m apart. The soil was a loamy sand.  
16 More information on the design, the lay-out and the management of the plantation can be found  
17 in Broeckx et al. (2012) and Berhongaray et al. (2015).

18 The part of the plantation in which this study took place was coppiced for the second time in  
19 March 2014. The poplar stems were cut manually about 10 cm above the soil surface. The  
20 experimental set-up of the automated GHG flux monitoring inter-comparison campaign is  
21 shown in Fig. 1A and 1B. The measurement set-up consisted of eight automated chambers  
22 located only in wide rows due to their size (AGPS, UIT Umwelt- und Ingenieurtechnik GmbH  
23 Dresden, Germany), eight automated chambers which were evenly distributed in narrow and  
24 wide rows (LI-8100A, LI-8150, LI-8100-104, LI-COR Biosciences, Lincoln, NE, USA), and  
25 eight soil gas concentration profile plots – each consisting of two soil gas samplers (ML 131099,  
26 Mikrolab, Højbjerg, Denmark) – which were also evenly distributed in narrow and wide rows.  
27 A detailed description of each soil GHG sampling device is presented in sections 2.2 and 2.3  
28 below. The inter-comparison campaign took place from 15 April 2014 until 31 August 2014.  
29 During this period the coppiced poplar stools regrew to a height of about 3.40 m. Canopy  
30 closure was achieved at the beginning of July 2014.

## 1 **2.2 Automated soil flux chamber systems**

2 The Greenhouse Gas Monitoring System AGPS (UIT Umwelt- und Ingenieurtechnik GmbH  
3 Dresden, Germany) and the LI-8100A Automated Soil CO<sub>2</sub> Flux System (LI-COR Biosciences,  
4 Lincoln, NE, USA) were both closed dynamic chamber systems with the chambers operating  
5 in sequence. The technical specifications of the two chamber systems are displayed in Table 1,  
6 and Fig. 1C shows a close-up of an AGPS chamber and a LI-8100A chamber.

7 The AGPS chambers ran on rails and were moved to and from the collar by an attached steel  
8 cable. The average time for closing the chamber was about 40 s. Once closed, the chamber  
9 rested directly on the collar rim. The tubing inlet and outlet went through one of the collar walls  
10 and were positioned 5 cm above the soil surface inside the measurement plot together with a  
11 non-shaded air temperature sensor. This design caused additional disturbance of the soil during  
12 collar installation because a small hole had to be dug in one corner of the measurement plot to  
13 put the tubing and the sensor cable into the ground. Each chamber was equipped with a  
14 combined soil sensor for temperature and moisture at 5 cm depth outside the collar. The  
15 chambers were connected to a multiplexer which was housed in an air-conditioned box (2.10  
16 m length x 1.21 m wide x 1.55 m high, 20 – 23 °C). Air was circulated in a closed loop between  
17 the chambers and the multiplexer with a pump installed inside the multiplexer. For gas  
18 concentration analyses, gas analysers were connected in a small closed loop with the  
19 multiplexer, continuously subsampling from the big sample loop with their own internal pump.  
20 Any type and number of gas analysers could be connected to the multiplexer in parallel as long  
21 as their combined flow rate did not exceed 2.5 l min<sup>-1</sup>. The AGPS can be bought pre-configured  
22 as described in the introduction, but for this study, the entire AGPS set-up had been completely  
23 custom-designed by UIT (Umwelt- und Ingenieurtechnik GmbH Dresden, Germany), including  
24 all the specifications listed in Table 1. Not included in the set-up were the gas analysers. Here,  
25 we report CO<sub>2</sub> data measured by a Fast Greenhouse Gas Analyser (FGGA, Los Gatos Research,  
26 Mountain View, CA, USA). All data were logged on a central computer and managed with the  
27 software SENSOWeb (UIT Umwelt- und Ingenieurtechnik GmbH). The computer was also the  
28 access point for remotely controlling the AGPS and the FGGA. The AGPS had continuously  
29 been deployed in the poplar plantation since May 2013 and was only shortly removed during  
30 the harvest (January - March 2014). Reinstallation of the AGPS took place during the first half  
31 of March 2014 in exactly the same locations that were used prior to the coppice operation. Due  
32 to extensive problems with condensing water inside the tubes in 2013, the tubing was equipped

1 with a heating system during reinstallation. During the flux monitoring, weeds were manually  
2 removed from inside the collars and around the chambers about every two weeks.

3 The AGPS sampling protocol consisted of the following steps: (i) 30 min tube heating, (ii) 5  
4 min sampling of atmospheric air at 50 cm height outside the multiplexer for flushing the gas  
5 analyser, (iii) 2 min purging of the tubes between the chamber and the multiplexer, (iv) 1 min  
6 in which the chamber closed, the multiplexer pump automatically turned off during this time,  
7 (v) 10 min measurement with 1 Hz gas sampling frequency, (vi) 1 min in which the chamber  
8 opened (multiplexer pump turned off), (vii) step ii repeated for 11 min. Each chamber was  
9 sampled every 4 hrs resulting in total in 48 measurements per day. The chambers did not move  
10 when the air temperature dropped below 2 °C (built-in freeze protection).

11 The LI-8100A Automated Soil CO<sub>2</sub> Flux System was an off-the-shelf product. It consisted of  
12 three main components: the gas analyser hosted in an analyser control unit (LI-8100A), a  
13 multiplexer (LI-8150), and the automated long-term chambers (8100-104) (LI-COR  
14 Biosciences, 2010). Both the analyser control unit and the multiplexer had their own weather-  
15 proof casing, requiring no additional air-conditioning. Neither tube heating nor freeze  
16 protection had been implemented; chambers operated at subzero temperatures. The chambers  
17 were moved by a non-flexible arm. The time needed to close a chamber was between 11 and  
18 15 s during which the multiplexer pump did not turn off. Once closed, the chamber did not rest  
19 directly on the collar rim, but on a metal plate surrounding the collar, leaving the collar  
20 undisturbed. Tubing inlet and outlet were installed inside the chamber. Soil sensors were  
21 installed the same way as for the AGPS. All measurement data were stored inside the analyser  
22 control unit on a compact flash card which could be accessed and controlled remotely via the  
23 central computer. The measurement protocol for each chamber consisted of a 2 min tubing pre-  
24 purge period, a 3 min measurement with 1 Hz gas sampling frequency, and 2 min tubing post-  
25 purge time. Each chamber was sampled every 2 hrs. The LI-8100A had been running at a  
26 different location in the plantation since March 2011 (Verlinden et al., 2013), and received a  
27 factory check-up in spring 2014. Reinstallation after the harvest took place at the beginning of  
28 March 2014. Weeding in and around the chambers followed the same routine as for the AGPS.

### 29 **2.3 Soil CO<sub>2</sub> concentration measurements**

30 Each soil CO<sub>2</sub> concentration sampler consisted of a 16 mm thick, corrosion-resistant steel tube  
31 with a 10 ml sampling cell (12 mm diameter) at its lower end. The length of the sampler

1 depended on the sampling depth. The sampling cell was connected to the surrounding soil via  
2 a 3 mm diameter opening in the steel tube. The opening was covered with a 12 x 0.5 mm<sup>2</sup>  
3 silicone disc to allow only the diffusion of gases between the soil and the cell. For sampling,  
4 the steel tube contained two smaller tubes made from stainless steel needles (18G, inner  
5 diameter 0.8–0.875 mm) which connected the sampling cell with the soil surface after  
6 installation (ML 131099, Mikrolab, Højbjerg, Denmark). The samplers were installed by pre-  
7 drilling a hole of the same diameter as the sampler to about 5 cm above the intended  
8 measurement depth. The samplers were inserted into the hole and carefully pushed to the  
9 measurement depth, aided by a 30 mm long, hardened PVC tip at the bottom of the sampler. At  
10 each soil gas concentration profile plot, two samplers were installed – one at 5 and one at 15  
11 cm depth.

12 Soil CO<sub>2</sub> was sampled about every two weeks between 10:00 and 14:00. A plastic syringe  
13 containing 10 ml N<sub>2</sub> and 50 ppm C<sub>2</sub>H<sub>4</sub> was connected via a two-way valve to one of the small  
14 tubes inside the sampler. An empty 10 ml glass syringe (SIGMA-ALDRICH, Diegem,  
15 Belgium) and a 12 ml pre-evacuated exetainer (Labco Ltd, Lampeter, UK) were connected to  
16 the other tube via a three-way valve. The N<sub>2</sub>/C<sub>2</sub>H<sub>4</sub> mixture was injected into the diffusion cell  
17 flushing the 10 ml soil gas sample via the second tube into the glass syringe. The glass syringe  
18 was then emptied into the exetainer. At last, 12 ml N<sub>2</sub> were injected into the exetainer to create  
19 an overpressure needed for the subsequent gas analysis. The concentration of C<sub>2</sub>H<sub>4</sub> recovered  
20 in the collected sample was used to calculate the dilution of the original sample which occurred  
21 while replacing it with N<sub>2</sub> in the sampling cell, and to correct the measured CO<sub>2</sub> concentration  
22 accordingly. The correction was performed with the assumption that there was full equilibrium  
23 between the diffusion cell and the inlet and outlet tube. During the sampling, diffusive loss of  
24 C<sub>2</sub>H<sub>4</sub> via the silicone membrane to the soil atmosphere was considered negligible. After the  
25 sampling, the diffusion cell and the sampling tubes were flushed with 60 ml N<sub>2</sub> to remove  
26 remaining traces of C<sub>2</sub>H<sub>4</sub>. For more details on the sampler design and the C<sub>2</sub>H<sub>4</sub> correction see  
27 Petersen (2014).

28 The gas samples were analysed on a Bruker Custom Greenhouse Analyser (Bruker Daltonik  
29 GmbH, Bremen, Germany) equipped with a thermal conductivity detector (TCD) for the  
30 analysis of CO<sub>2</sub> and C<sub>2</sub>H<sub>4</sub>. The TCD channel was equipped with a Hayesep column.  
31 Temperatures of the inlet, column and TCD were 50, 50 and 200 °C, respectively. Helium at 20  
32 ml min<sup>-1</sup> was used as reference flow. Total flow was 60 ml min<sup>-1</sup>. Concentrations were

1 quantified with reference to three calibration gases with an accuracy of 2 %: (i) 50  $\mu\text{l l}^{-1}$   $\text{C}_2\text{H}_4$   
2 in  $\text{N}_2$ , (ii) 799  $\mu\text{l l}^{-1}$   $\text{CO}_2$  in synthetic air, and (iii) 5.04 %  $\text{CO}_2$  in synthetic air.

### 3 **2.4 Soil sampling**

4 To assess the impact of the permanently installed chambers on soil properties which potentially  
5 control soil  $\text{CO}_2$  concentrations and flux rates, as well as to assess the comparability between  
6 the flux measurement plots, soil samples were taken before and after the inter-comparison  
7 campaign. In February 2014, undisturbed topsoil samples were taken along two transects (Fig.  
8 1A). At each transect, three samples were taken per row type and per sampling depth. For soil  
9 C and dissolved organic carbon (DOC), soil was sampled at 0-10 and 10-20 cm depth with an  
10 auger ( $\sim 2$  cm diameter). Separate samples were taken with stainless steel cylinders (100  $\text{cm}^3$ )  
11 (Eijkelkamp Agrisearch equipment, Giesbeek, The Netherlands) at 0-5 and 10-15 cm depth for  
12 dry bulk density. Soil sampling was repeated at the beginning of September 2014, but this time  
13 in each of the 16 chamber collars and within each soil gas sampling plot.

14 About 9 g field moist soil of each auger sample was shaken in 35 ml 0.5M  $\text{K}_2\text{SO}_4$  for 1 hr. This  
15 suspension was filtered with Whatman filter paper (grade 42, ashless, 150 mm) and the filtered  
16 liquid analysed for DOC with Continuous Flow Analysis (CFA) (San++ Automated Wet  
17 Chemistry Analyzer, Skalar Analytical, Breda, The Netherlands). The rest of the auger samples  
18 were dried at 50  $^\circ\text{C}$ , ground and three subsamples per sample were analysed by dry combustion  
19 with a NC element analyser (NC-2100, Carlo Erba Instruments, Italy) and means reported. Out  
20 of necessity the February 2014 samples had to be aggregated by row type and sampling depth  
21 prior to the grinding. The steel cylinder samples were dried at 105  $^\circ\text{C}$  to constant weight for dry  
22 bulk density determination.

23 The soil data from February 2014 were grouped by row type, and the data from September 2014  
24 by row type and measurement device. One-way omnibus ANOVA and the Tukey Honest  
25 Significant Difference test were used to compare group means ( $\alpha = 0.05$ ). Normality for each  
26 group and homogeneity of variance of the groups were tested with the Shapiro-Wilk test and  
27 the Levene test, respectively. The soil data analysis as well as any other data analysis for this  
28 study were conducted with the software R (version 3.1.1) (R Core Team, 2014). The only  
29 exception was the chamber flux calculation for the AGPS (section 2.5) which had to be  
30 conducted with R version 3.0.2 due to a package incompatibility.



## 1 **2.5 Chamber flux calculation and quality control**

2 For the AGPS, descriptive statistics and water-corrected CO<sub>2</sub> fluxes were calculated with a self-  
3 written R script incorporating the “gasfluxes” script (Roland Fuß, Institute of Agricultural  
4 Climate Research, Johann Heinrich von Thünen Institute, Braunschweig, Germany, version  
5 0.98.int) and the HMR package (Pedersen et al., 2010), and additionally by employing the  
6 packages “zoo”, “xts” and “xtsExtra” (Zeileis and Grothendieck, 2005; Ryan and Ulrich, 2014;  
7 Weylandt, 2014). For each AGPS measurement, the flux was calculated with linear regression,  
8 robust linear regression with a Huber-M estimator (RLM) (Huber, 1981), and a modified  
9 Hutchinson-Mosier non-linear function (HMR) (Pedersen et al., 2010). This procedure was  
10 performed twice for each measurement – for a closure time of 4 min and 9 min, respectively.  
11 Prior to each flux calculation, the first minute of the CO<sub>2</sub> concentration curves was discarded  
12 (= deadband) to account for the time needed to establish steady headspace mixing as well as  
13 any disturbances caused by the chamber placement at the beginning of the measurement  
14 (Christiansen et al., 2011; Koskinen et al., 2014). For each flux calculation, the “gasfluxes”  
15 script selected the HMR flux if (i) the Akaike information criterion (AIC) of HMR was smaller  
16 than the AIC of the linear fit, (ii) the *p*-value of the flux calculated with HMR was smaller than  
17 the *p*-value of the flux calculated with linear regression, and if (iii) the flux calculated with  
18 HMR was not more than four times higher/lower than the flux calculated with RLM. In all other  
19 cases, RLM was chosen as the best-fitting model. The fluxes calculated by linear regression  
20 and RLM were the same, except that RLM was robust against outliers in the CO<sub>2</sub> concentration  
21 curves. Fluxes were converted from  $\mu\text{l m}^{-2} \text{s}^{-1}$  to  $\mu\text{mol m}^{-2} \text{s}^{-1}$  using the ideal gas law (Parkin  
22 and Venterea, 2010) with air temperature and pressure provided by the AGPS and the LI-  
23 8100A, respectively.

24 For the LI-8100A, water-corrected mass CO<sub>2</sub> fluxes and descriptive statistics were  
25 automatically provided by the LI-8100 File Viewer Version 3.0.0 (LI-COR Biosciences). For  
26 each chamber measurement, the flux was either calculated with a linear or an empirical  
27 exponential regression (LI-COR Biosciences, 2010). The software compared for each  
28 measurement the normalized sums of the squares of the residuals (SSN) of the linear and the  
29 exponential fit to find the best-fitting model. The first 25 s of each 3 min CO<sub>2</sub> concentration  
30 curve were discarded before the flux calculation.

31 Fluxes were discarded from the two datasets by applying in sequence the following quality  
32 control criteria: (i) negative fluxes, (ii) fluxes with the SSN of the linear fit > 1.0 ppm CO<sub>2</sub>

1 (equivalent to a root mean square error threshold of 1.0 ppm CO<sub>2</sub>, Görres et al., 2014), (iii)  
 2 decrease in headspace temperature during the closure time by more than 0.5 °C or increase by  
 3 more than 1.0 °C, (iv) difference in the atmospheric CO<sub>2</sub> concentration 5 cm above the collar  
 4 directly before the chamber closure and after a deadband of 1 min of less than 0.0 ppm (i.e.  
 5 decreasing CO<sub>2</sub> concentration), and (v) mean relative humidity (RH) inside the closed chamber  
 6 higher than 100 %. The first criterion detected chamber measurements with large leaks, whereas  
 7 smaller leakages and other measurement disturbances could be detected by selecting an  
 8 appropriate noise level threshold in the second criterion. CO<sub>2</sub> flux measurements can be very  
 9 sensitive to changes in environmental conditions, thus criteria (iii) – (v) removed measurements  
 10 for which the CO<sub>2</sub> concentration increase curve looked okay, but which might still have been  
 11 biased by changes in environmental conditions too large to guarantee continuous identical  
 12 diffusion conditions during chamber closure.

## 13 **2.6 Soil diffusivity and gradient-based CO<sub>2</sub> flux calculation**

14 Changes in topsoil CO<sub>2</sub> concentration dynamics for each collar and each soil gas sampling plot  
 15 throughout the inter-comparison campaign were approximated by calculating the effective soil  
 16 diffusion coefficient ( $D_s$ ) which is the product of the CO<sub>2</sub> diffusion coefficient in free air ( $D_a$ )  
 17 and the gas tortuosity factor  $\zeta$ .  $D_a$  was corrected for temperature and air pressure by

$$18 \quad D_a = D_{a0} \left( \frac{T}{293.15} \right)^{1.75} \left( \frac{P}{101.3} \right) \quad (1)$$

19 where  $T$  is soil temperature at 5 cm depth (K),  $P$  the air pressure from the LI-8100A (kPa), and  
 20  $D_{a0}$  a reference value of  $D_a$  at 20 °C (293.15 K) and 101.3 kPa given as 14.7 mm<sup>2</sup> s<sup>-1</sup> (Jones,  
 21 1992). The empirical Millington-Quirk model was used for estimating  $\zeta$  (Millington and Quirk,  
 22 1961):

$$23 \quad \zeta = \frac{(\phi - \text{VWC})^{10/3}}{\phi^2} \quad (2)$$

24 where VWC is the volumetric water content at 5 cm depth and  $\phi$  the total porosity (m<sup>3</sup> m<sup>-3</sup>).  
 25 Total porosity was calculated by dividing the averaged topsoil dry bulk density for each  
 26 measurement plot by the particle density. Particle density was empirically adjusted for the C  
 27 content at each measurement plot according to eq. 12 in Rühlmann et al. (2006), assuming a C  
 28 content in the organic matter of 55 %.

1 Additionally, soil CO<sub>2</sub> fluxes were calculated via Fick's first law of diffusion by multiplying  
2 the CO<sub>2</sub> concentration gradients between 5 and 15 cm depth obtained from the soil gas sampling  
3 plots with the respective  $D_s$  (Roland et al., 2015). Prior to the flux calculation, soil CO<sub>2</sub>  
4 concentrations in ppm were converted to  $\mu\text{mol m}^{-3}$  by multiplying them by the molar volume  
5 of a gas at standard temperature and pressure ( $0.04462 \mu\text{mol L}^{-1}$ , Brummell and Siciliano,  
6 2011). Soil temperature and soil moisture values at 5 cm depth were obtained from the nearest  
7 chamber in the same row type.

## 8 **2.7 Comparison of the CO<sub>2</sub> flux datasets**

9 The AGPS and LI-8100A soil CO<sub>2</sub> fluxes were directly compared for four different  
10 environmental conditions, namely (i) daytime, constant atmospheric CO<sub>2</sub> concentration, (ii)  
11 daytime, fluctuating atmospheric CO<sub>2</sub> concentration, (iii) nighttime, constant atmospheric CO<sub>2</sub>  
12 concentration, and (iv) nighttime, fluctuating atmospheric CO<sub>2</sub> concentration. Daytime and  
13 nighttime fluxes were separated based on local sunrise and sunset times. Atmospheric CO<sub>2</sub>  
14 concentration was considered as constant when the CO<sub>2</sub> concentration measured at 50 cm height  
15 above the soil surface had a standard deviation  $< 1.0$  ppm (3 min measurements). Constant  
16 ambient CO<sub>2</sub> concentrations were seen as a proxy indicator of a well-mixed atmosphere, i.e.  
17 wind perturbation.

18 Additionally, two modelling approaches were applied for the comparison of the two flux  
19 datasets. Firstly, average CO<sub>2</sub> flux rates for each automated chamber system and their respective  
20 95 % confidence intervals were estimated using generalized additive models (GAM) with a  
21 nonlinear smooth (thin plate regression spline) for time and with random smooths (factor  
22 smooth interactions) over time for each chamber (R packages 'itsadug' and 'mgcv', function  
23 'bam') (Wood, 2006; van Rij et al., 2015). Autocorrelation was accounted for by including an  
24 AR1 model. Input data were the unfiltered and filtered CO<sub>2</sub> fluxes, respectively, averaged by  
25 day and by chamber. Secondly, the chamber flux datasets were quantitatively compared by  
26 using the common approach of modelling SR according to Lloyd and Taylor (1994) (eq. 11):

$$27 \text{ SR} = R_{10} \exp E_0 \left( \frac{1}{56.02} - \frac{1}{T-227.13} \right) \quad (3)$$

28 where  $R_{10}$  is the respiration rate at 10 °C ( $\mu\text{mol CO}_2 \text{ m}^{-2} \text{ s}^{-1}$ ),  $E_0$  the temperature sensitivity  
29 coefficient (K), and  $T$  the soil temperature at 5 cm depth (K). SR was modelled separately for  
30 each combination of chamber system and row type. Each model was also fitted once with the  
31 unfiltered and the filtered dataset, respectively, using nonlinear regression (R function 'nls').

1 Input data were the single measured CO<sub>2</sub> fluxes. A part of the chamber measurements were  
2 excluded from the modelling due to missing soil temperature values (sensor malfunctions).  
3 Cumulated CO<sub>2</sub> fluxes for the monitoring period were calculated by running the different fitted  
4 SR models with average hourly time series of soil temperature at 5 cm depth. For the  
5 construction of the average hourly time series, the time series with the least number of gaps was  
6 chosen as a reference to which all other chamber soil time series were linearly correlated. Any  
7 remaining gaps in the time series were linearly interpolated and the time series subsequently  
8 averaged for each combination of chamber system and row type. Model runs were performed  
9 with the R function 'predictNLS' (package 'propagate') which calculated 95 % confidence  
10 intervals for the fitted values by using Monte Carlo simulation and taking into account the error  
11 in the model parameter estimates as well as the standard deviation of the averaged soil  
12 temperature time series.

13

### 14 **3 Results**

#### 15 **3.1 Variability in environmental conditions**

16 In February 2014 the dry bulk density in the undisturbed top soil was  $1.41 \pm 0.11$  g cm<sup>-3</sup> dry soil<sup>-1</sup>  
17 (average  $\pm$  STD, n=24), the C content  $1.21 \pm 0.17$  % (n=8, pre-analysis sample pooling), and  
18 the DOC content  $32.07 \pm 10.03$   $\mu$ g g<sup>-1</sup> dry soil<sup>-1</sup> (n=24), with no significant differences between  
19 wide and narrow poplar rows. The soil sampling results at the end of the chamber inter-  
20 comparison campaign did not differ significantly from these values. After the end of the flux  
21 monitoring, the inner walls of the LI-8100A collars were covered with a loose mat of new  
22 grown roots (Fig. A, supplementary material). Such a mat was not observed during the removal  
23 of the AGPS chambers and soil gas samplers. However, no significant differences in dry bulk  
24 density, C, and DOC between the devices were found within a row type. Between row types,  
25 only the dry bulk density inside the AGPS collars in the wide rows ( $1.44 \pm 0.07$  g cm<sup>-3</sup> dry soil<sup>-1</sup>  
26 <sup>1</sup>, n=16) differed significantly from the LI-8100A chambers ( $1.32 \pm 0.12$  g cm<sup>-3</sup> dry soil<sup>-1</sup>, n=8)  
27 and the soil gas samplers ( $1.24 \pm 0.13$  g cm<sup>-3</sup> dry soil<sup>-1</sup>, n=5) installed in the narrow rows. Thus,  
28 a methodological comparison of the soil CO<sub>2</sub> flux dynamics captured by the flux measurement  
29 devices within a row type was regarded as feasible.

30 Air-filled porosity and the derived soil diffusion coefficient showed a high variability  
31 throughout the monitoring time. They were on average slightly higher in the narrow rows than

1 in the wide rows (Fig. 2A and 2B). This variability was driven by several heavy rain events  
2 resulting in sharp soil moisture increases (Fig. 2C). From July 2014 onwards standing water  
3 was observed in parts of the wide rows following precipitation, but never in the narrow rows  
4 which drained much faster despite no significant differences in dry bulk density between row  
5 types.

6 The AGPS collars received more direct sunlight than the LI-8100A collars, resulting in higher  
7 air and subsequently constantly higher soil temperatures (Fig. 2D). This was an effect of the  
8 weeding since the collar area which could be potentially shaded by the vegetation still  
9 surrounding the chamber decreased with increasing collar area. The average daily soil  
10 temperature difference between the AGPS and the LI-8100A was generally less than 1 °C when  
11 the fraction of shading by the vegetation was homogenous throughout the study site. However,  
12 during the transition period from an open to a closed poplar canopy the soil temperature  
13 difference was constantly higher than 1 °C. This transition period from the beginning of June  
14 until the middle of July also coincided with the warmest and the driest monitoring period.  
15 Canopy closure above the AGPS collars was reached about a week later in comparison to the  
16 LI-8100A chambers because the larger structure of the AGPS chambers hindered the growing  
17 poplar stems from leaning towards each other (see Fig. B in the supplementary material for the  
18 different vegetation stages). The high air temperatures observed above the AGPS collars were  
19 also partly an artefact of the non-shaded sensors. During a small proportion of the AGPS  
20 measurements, the temperature inside the chamber decreased by more than 0.5 °C (Fig. 3). This  
21 phenomenon was mainly observed above an ambient air temperature of 20 °C and was regarded  
22 as an indicator for the cooling down of an overheated sensor. Overall, the insulation of the  
23 chambers worked well, with more than 68 % and 80 % of the AGPS and LI-8100A  
24 measurements, respectively, fulfilling quality control criterion 3.

25 Variability in air and soil temperature decreased after the canopy closure at the beginning of  
26 July, but the opposite was true for the atmospheric CO<sub>2</sub> concentration measured 50 cm above  
27 the soil surface. Constant atmospheric CO<sub>2</sub> concentrations at that height were only observed  
28 before the canopy closure and mainly during daytime as one would expect with a well-mixed  
29 boundary atmosphere (= instable atmospheric layering). For more than 70 % of the flux  
30 measurements, the atmospheric CO<sub>2</sub> concentration 50 cm above the soil surface fluctuated by  
31 more than 1.0 ppm prior to the chamber closure. Atmospheric CO<sub>2</sub> concentrations measured 5  
32 cm above the collars at the time of chamber closure matched well between the AGPS and the

1 LI-8100A most of the time (Fig. 2E). However, the AGPS recorded a number of atmospheric  
2 CO<sub>2</sub> concentrations at chamber closure above 500 ppm which were not observed by the LI-  
3 8100A. Two-thirds of the AGPS CO<sub>2</sub> values above 500 ppm were measured during nighttime.

### 4 **3.2 Technical reliability of the two chamber systems**

5 During the inter-comparison campaign, the LI-8100A conducted 12874 chamber measurements  
6 (wide rows: 6253, narrow rows: 6621) of which only 1 measurement had to be discarded due  
7 to technical problems with the chamber closing mechanism. Overall, the LI-8100A showed a  
8 high robustness despite having previously operated continuously in the poplar plantation for  
9 three years. It recorded only 62 suspicious atmospheric air pressure readings and 206 readings  
10 of RH inside the closed chambers of more than 100%, indicating conditions of water  
11 condensation. The AGPS conducted 78 % of the theoretically possible 6296 chamber  
12 measurements. A negligible amount of measurements did not take place due to system  
13 maintenance (n=37), activation of the freeze protection (n=10) and chamber malfunctions  
14 (n=111). Chamber malfunctions were all caused by the steel cables which moved the AGPS  
15 chambers. These cables did expand or contract depending on the air temperature, and as a  
16 consequence, their tension had to be checked and corrected once per week or at least every two  
17 weeks to prevent chambers from getting stuck.

18 Two main issues prevented the AGPS from operating continuously in the field. First, the air  
19 filters inside the multiplexer became clogged up with liquid water during heavy rain events,  
20 preventing 602 potential measurements. That could have probably been avoided if the inlets at  
21 the collars would have been equipped with air filters the same way as LI-8100A chambers are.  
22 Secondly, 609 chamber measurements could not be analysed because the gas analyser froze.  
23 Each time these two issues occurred, it was possible to get the AGPS operational again in less  
24 than 2 hr. The large amount of lost data was mainly attributable to the fact that most of the time  
25 someone had to be present in the field for maintenance which was not always possible on the  
26 very day the problems occurred.

27 Another issue with the gas analyser was that the internal software did not save the measured  
28 data continuously at 1 Hz. For the 4 min closure time and the 9 min closure time only 1070 (22  
29 %) and 328 (7 %) measurements provided a dataset at 1 Hz frequency, respectively. The median  
30 number of data points for the short and long flux calculation period (i.e. chamber closure time

1 excl. 1 min deadband period) was 167 and 328, respectively. During the first half of June 2014,  
2 the number of data points per measurement even dropped below 50 and 100, respectively.

### 3 **3.3 Flux quality**

4 In total 23 % of the LI-8100A CO<sub>2</sub> flux measurements were discarded, mainly because of  
5 headspace temperature changes (Table 2). During the open canopy phase, this problem was  
6 mainly encountered during the day, whereas equal amounts of fluxes were discarded from the  
7 daytime and nighttime dataset based on headspace temperature changes once the canopy was  
8 closed. With respect to row type, headspace temperature problems were more often encountered  
9 in the wide rows, whereas chamber measurements in the narrow rows were more likely to have  
10 a  $SSN_{Lin} > 1.0$  ppm or a RH > 100 % than those in the wide rows. More than 50 % of the LI-  
11 8100A concentration curves were best-fitted exponentially, especially under fluctuating  
12 atmospheric CO<sub>2</sub> concentrations.

13 For the AGPS dataset, a higher proportion of the concentration curves were best-fitted linearly  
14 regardless of daytime or atmospheric CO<sub>2</sub> concentration variability. Only for the 4 min closure  
15 time in the filtered dataset were the two flux calculation models about equally distributed. In  
16 total, 71 and 94 % of the AGPS fluxes using the short and the long flux calculation period,  
17 respectively, did not pass the quality control (Table 2). No correlation was found between the  
18 amount of discarded data and the tubing length of the chambers. For the unfiltered dataset, the  
19 fluxes calculated for 9 min closure time were  $0.21 \pm 0.50 \mu\text{mol m}^{-2} \text{s}^{-1}$  (average  $\pm$  STD) lower  
20 than the fluxes calculated for a 4 min closure time. In the filtered dataset, this was reduced to  
21  $0.18 \pm 0.18 \mu\text{mol m}^{-2} \text{s}^{-1}$ . Due to the low data quality for the long flux calculation period, only  
22 the fluxes calculated for the 4 min closure time were considered in the remaining result sections  
23 below.

24 For the 4 min closure time, 2882 flux measurements had a  $SSN_{Lin} > 1.0$  ppm. This included  
25 almost all data from the first half of June where we had the severe gas analyser logging problem.  
26 The  $SSN_{Lin}$  criterion also already filtered out 60 % and 79 % of the flux measurements with  
27 headspace temperature problems and with a decrease of the CO<sub>2</sub> headspace concentration  
28 during the deadband period, respectively. The latter criterion filtered out most of the flux  
29 measurements which had shown a large discrepancy in initial chamber CO<sub>2</sub> concentration as  
30 compared to the LI-8100A in Fig. 2E. Measurements which did not pass this criterion had a  
31 median pre-closure atmospheric CO<sub>2</sub> concentration at 5 cm height above the collar of 600 ppm,

1 whereas measurements passing this criterion had a median pre-closure atmospheric CO<sub>2</sub>  
2 concentration of 433 ppm.

3 The SSN<sub>Lin</sub> criterion would have also detected 83 % of the negative CO<sub>2</sub> fluxes. Negative CO<sub>2</sub>  
4 fluxes were clearly associated with severely leaking chambers. Insufficient airtight sealing was  
5 also probably a problem for a part of the fluxes with a high SSN<sub>Lin</sub>. In contrast to the LI-8100A  
6 chambers, the AGPS chambers had no mechanism which additionally pressed them onto the  
7 collar once the sealing and the collar rim came in contact. The AGPS chamber and the collar  
8 had to be perfectly aligned to achieve an airtight sealing which was challenging and required  
9 regular re-adjustments of the collars throughout the monitoring. However, the noise in the  
10 AGPS flux dataset was large regardless of the environmental conditions, and the noise was  
11 lower at constant atmospheric CO<sub>2</sub> concentrations, i.e. windy conditions. All of this pointed to  
12 an inherent technical problem with the system (see Discussion below).

### 13 **3.4 Comparison of the CO<sub>2</sub> flux datasets**

14 Until the beginning of July 2014, CO<sub>2</sub> concentrations at 5 and 15 cm depths in the narrow rows  
15 were 4702±762 ppm (average±SE, n=16) and 12565±2145 ppm (n=15), respectively, and in  
16 the wide rows 6664±1108 ppm (n=14) and 12251±1512 ppm (n=15), respectively. Afterwards,  
17 CO<sub>2</sub> concentrations increased at 5 and 15 cm depth in the narrow rows to on average  
18 11797±2365 ppm (n=20) and 27071±3615 ppm (n=19), respectively. In the wide rows, CO<sub>2</sub> at  
19 5 cm depth reached the same concentrations as in the narrow rows, whereas at 15 cm depth, it  
20 increased even further (38008±4574 ppm, n=19). The increasing steepness of the soil CO<sub>2</sub>  
21 concentration gradient was probably partly the result of CO<sub>2</sub> accumulation in the soil due to the  
22 reduced air-filled porosity as the magnitude of the surface CO<sub>2</sub> fluxes measured with the  
23 chambers did not increase strongly during this period (Fig. 4). Contrastingly, the CO<sub>2</sub> fluxes  
24 based on the flux gradient method were unrealistically high in July and August 2014 (wide row:  
25 8.9±1.5 μmol m<sup>-2</sup> s<sup>-1</sup>, n=19; narrow row: 10.8±1.5 μmol m<sup>-2</sup> s<sup>-1</sup>, n=17), whereas prior to the  
26 rewetting, they were in the same range as the chamber CO<sub>2</sub> fluxes (wide row: 2.6±0.5 μmol m<sup>-2</sup>  
27 s<sup>-1</sup>, n=12; narrow row: 3.9±0.6 μmol m<sup>-2</sup> s<sup>-1</sup>, n=15). The soil depth resolution chosen in this  
28 study for the flux gradient method was very likely too low to realistically approximate the soil  
29 CO<sub>2</sub> concentration profiles and soil diffusion coefficients during high soil moisture conditions.  
30 Short-term fluctuations in the soil CO<sub>2</sub> concentration profiles due to heavy precipitation events  
31 were unlikely to be the main cause for the failure of the flux gradient method in July and August



1 2014 because the soil CO<sub>2</sub> concentration samplings were performed at least three days after  
2 such events, except for the last sampling.

3 Daily average CO<sub>2</sub> fluxes estimated from the unfiltered flux datasets did not differ significantly  
4 between the two chamber systems, however, the daily AGPS flux rates tended to be lower than  
5 the flux rates obtained with the LI-8100A during the open canopy phase (Fig. 4, top panel).  
6 With regard to the single unfiltered CO<sub>2</sub> flux measurements, the dataset from the AGPS showed  
7 higher flux variability throughout the inter-comparison campaign than the unfiltered CO<sub>2</sub> flux  
8 dataset from the LI-8100A chambers installed in the same (wide) rows (Fig. 4). This difference  
9 in flux variability disappeared with the filtering except for a number of very low fluxes observed  
10 only by the AGPS during the open canopy phase (Fig. 5). In contrast to the AGPS, filtering  
11 mainly thinned out the LI-8100A dataset of the open canopy phase since the biggest problem  
12 for these chambers was overheating. LI-8100A chambers installed in the wide rows were more  
13 subjected to this problem than those in the narrow rows (Fig. C, supplementary material). The  
14 fit of the GAM for the LI-8100A dataset was only slightly changed by the filtering whereas the  
15 fit for the AGPS changed significantly. This led to a distinct separation of the two GAM curves  
16 for the daily CO<sub>2</sub> fluxes (Fig. 5, top panel) with the AGPS flux estimates being constantly lower  
17 in comparison to the LI-8100A. However, both chamber systems still seemed to be able to  
18 capture the same temporal flux dynamics although the AGPS model curve was slightly shifted  
19 to the right in comparison to the LI-8100A model curve.

20 Modelling CO<sub>2</sub> fluxes along the soil temperature gradient revealed discrepancies between the  
21 datasets of the AGPS and the LI-8100A similar to those visualized by the GAM. Filtering the  
22 LI-8100A dataset changed only slightly the model fits of the Lloyd and Taylor model and had  
23 no significant effect on the subsequently calculated SR balances (Table 3, Fig. 6). The opposite  
24 was observed for the AGPS dataset. The regression parameters based on the AGPS dataset were  
25 lower than the ones based on the LI-8100A dataset from the wide rows (Table 3); the  
26 discrepancies between the regression lines increased with increasing soil temperature and the  
27 data filtering (Fig. 6). Similar SR balances and R<sub>10</sub> values were only obtained by the two  
28 chamber systems during the closed canopy phase. Regardless of chamber type, row type and  
29 environmental conditions, the filtering led to a decrease in the SR balance estimates, but it also  
30 improved the model fit (see Fig. D in the supplementary material for the distribution of the  
31 residuals). The SSN<sub>Lin</sub> and the headspace temperature criteria filtered out fluxes mainly above  
32 1.5 μmol CO<sub>2</sub> m<sup>-2</sup> s<sup>-1</sup>. Only criterion (iv) mainly removed positive fluxes below 1.5 μmol CO<sub>2</sub>

1  $\text{m}^{-2} \text{s}^{-1}$ , but this criterion was not applicable to the LI-8100A chambers since these chambers  
2 did not provide an undisturbed pre-closure atmospheric  $\text{CO}_2$  concentration.

3 The tendency that the absolute differences in the  $\text{CO}_2$  flux rates between the two datasets varied  
4 throughout the monitoring period was also visible when looking just at the measurement periods  
5 with the highest data quality (Fig. 7). During the open canopy phase, the AGPS flux rates were  
6  $0.31 \pm 0.03 \mu\text{mol CO}_2 \text{ m}^{-2} \text{ s}^{-1}$  (average  $\pm$  SE,  $n=47$ ) lower than the ones obtained by the LI-8100A,  
7 whereas during the closed canopy phase, the opposite was observed with the AGPS flux rates  
8 being  $0.08 \pm 0.06 \mu\text{mol CO}_2 \text{ m}^{-2} \text{ s}^{-1}$  ( $n=15$ ) higher.

9

## 10 **4 Discussion**

11 The chamber methodology is based on the simple principle of diffusion, but it is an invasive  
12 method and seemingly small changes in the chamber design, the measurement protocol and the  
13 data analysis can lead to significant biases in the measured fluxes (Davidson et al., 2002; de  
14 Klein and Harvey, 2012). These biases have been quantified for different chamber types under  
15 controlled laboratory conditions, and this has already led to significant improvements in the  
16 methodology (Pumpanen et al., 2004; Christiansen et al., 2011; Pihlatie et al., 2013). However,  
17 laboratory tests have the drawback that they can only cover a limited and simplified set of  
18 environmental conditions. The field site of this study offered the unique possibility to study the  
19 chosen automated chamber systems in a wide range of environmental conditions within a short  
20 period of time. The following sections are going to address real alterations of the field SR  
21 introduced by the presence of the chamber systems, by measurement artefacts caused by  
22 environmental conditions that affect chamber performance, and by biases introduced by the  
23 subsequent data analysis.

### 24 **4.1 Effect of chambers on environmental conditions**

25 The impact of the automated chamber systems on the vegetation structure increased with the  
26 size of the chamber itself and additionally with the size of the frame needed for the support and  
27 the movement of the chamber. To guarantee unrestricted movement and air-tight closure of  
28 automated chambers, the support structure has to be kept free of vegetation. Additionally, the  
29 height of the chambers restricts the height to which vegetation can be allowed to grow inside  
30 the collars. At the poplar plantation, this subsequently altered the environmental conditions for  
31 each chamber system in two ways. First, the smaller LI-8100A was able to cover a wider range

1 of environmental conditions since it could also be installed in the narrow rows. Including the  
2 narrow rows increased the overall SR balance of the site obtained by the LI-8100A flux  
3 measurements by about 20 %. Soil respiration at this site was higher in the narrow rows as  
4 compared to the wide rows due to the higher fine root biomass and better aeration (Verlinden  
5 et al., 2013). Secondly, the larger size of the AGPS chambers required more weeding, and it  
6 also prevented the resprouting poplar stems to lean towards each other early in the growing  
7 season, thus slightly delaying canopy closure. The resulting reduced shading made a larger  
8 proportion of the measurement plot susceptible to soil heating and drying, but also precipitation  
9 events had a more immediate effect on the soil surface since less precipitation was intercepted  
10 by the vegetation canopy (lower leaf area index) in comparison to the LI-8100A. Biological  
11 processes in the soil have temperature and moisture optima (Schipper et al., 2014; Zhou et al.,  
12 2014). Thus, differences in temperature and moisture can have led either to lower or higher SR  
13 fluxes from the AGPS in comparison to the LI-8100A depending on the time of the  
14 measurement. However, it is not possible to resolve these differences in more detail in this  
15 study.

16 Potential alterations of environmental conditions due to the presence of automated chamber  
17 systems are not restricted to the aboveground part of the ecosystem. A problem shared by  
18 manual and automated chambers is the effect of the collar presence on soil conditions. During  
19 installation, collars can cut roots and disturb the soil structure, leading to significant alterations  
20 of SR fluxes. The risk of altering SR dynamics increases with collar insertion depth. However,  
21 the common consensus in the literature is that these disturbances are only temporary and can  
22 be largely overcome by installing the collars long before the actual start of the chamber  
23 measurements (Hutchinson and Livingston, 2001; Davidson et al., 2002; de Klein and Harvey,  
24 2012). The current recommendation for minimising disturbance of environmental conditions  
25 by the presence of automated chambers is to have at least two collars per replicate plot and to  
26 move the chambers regularly between the collars. It does not include the regular relocation of  
27 the collars itself (de Klein and Harvey, 2012). To our knowledge we are the first to report the  
28 restriction of horizontal root growth by collars and the subsequent build-up of root mats along  
29 the interior collar walls. Root respiration is an important component of the total SR flux (Vargas  
30 et al., 2011; Heinemeyer et al., 2011). The development of root mats only in the LI-8100A  
31 collars, which had a deeper insertion depth than the AGPS collars, might have contributed to  
32 the higher SR observed in the wide rows by the LI-8100A in comparison to the AGPS. The  
33 small size of the LI-8100A chambers allows the system to cover a wider range of microsites in

1 the field and it makes it easy to relocate the chambers. However, the contribution of any type  
2 of collar edge effect to the total SR flux increases with an increasing collar perimeter to collar  
3 area ratio, and is thus more of a problem for smaller chambers.

#### 4 **4.2 Effect of environmental conditions on chamber performance**

5 Collars have the purpose to help provide an air-tight system during chamber measurements by  
6 (i) offering a smooth contact surface for the chamber to rest on which can be sealed using either  
7 rubber or water seals, and by (ii) preventing lateral soil gas diffusion and thus leakages in the  
8 soil during chamber deployment (Hutchinson and Livingston, 2001). Chamber leakages can  
9 lead to negligible or significant flux underestimation depending on the environmental  
10 conditions and soil properties (Hutchinson and Livingston, 2001). For example, the collar  
11 insertion depth necessary to reduce the error due to lateral soil gas diffusion increases with  
12 increasing air-filled porosity (Hutchinson and Livingston, 2001; Heinemeyer and McNamara,  
13 2011; Creelman et al., 2013). The increase in soil CO<sub>2</sub> concentrations during the closed canopy  
14 phase in the poplar plantation which was not accompanied by a change of magnitude in the  
15 chamber CO<sub>2</sub> fluxes, and the unrealistic SR estimates obtained with the soil gradient flux  
16 method during this period, were indicative of a significant decrease in air-filled porosity and  
17 thus diffusivity (Turcu et al., 2005; Hashimoto and Komatsu, 2006). The application of the flux  
18 gradient method has been shown to be problematic in soils which are near water saturation  
19 because of the difficulties to estimate low soil diffusion coefficients with high certainty (Maier  
20 and Schack-Kirchner, 2014). The AGPS was more prone to lateral diffusive soil gas losses than  
21 the LI-8100A due to its shallower collar insertion depth. Thus, lateral soil gas diffusion losses  
22 likely played a significant role in the larger discrepancy observed in the SR estimates between  
23 the two automated chamber systems during the open canopy phase (before coppice) in  
24 comparison to the closed canopy phase with its higher soil moisture conditions.

25 Flux underestimation caused by leakages in the aboveground seal was certainly also an issue  
26 for the AGPS as could be seen from the high maintenance needs necessary to keep the seal  
27 properly aligned to the collar and the large noise in the dataset. The LI-8100A flux dataset had  
28 a very low noise level regardless of the wide range of environmental conditions encountered at  
29 the poplar plantation, especially regardless of the wind protection. This is a good indicator that  
30 the chambers had no issue with the airtightness of the rubber sealing. Under windy conditions,  
31 one can expect to see more noise in the CO<sub>2</sub> concentration curves obtained during chamber  
32 closure if the chamber seal is not perfectly airtight (Bain et al., 2005). However, the AGPS

1 dataset had a high noise level throughout the entire inter-comparison campaign, and it was  
2 highest during calm conditions. Additionally, high  $SSN_{Lin}$  values were often associated with  
3 higher fluxes ( $>1.5 \mu\text{mol CO}_2 \text{ m}^{-2} \text{ s}^{-1}$ ). These are indicators that the sample air flow rate between  
4 the multiplexer and the chambers was not high enough to sufficiently mix the chamber  
5 headspace during the measurements (Liu and Si, 2009; Christiansen et al., 2011). Insufficient  
6 headspace mixing leads also to flux underestimation (Liu and Si, 2009; Christiansen et al.,  
7 2011).

8 Chamber design-induced flux estimation errors can be reduced by shortening the chamber  
9 closure time (Venterea and Baker, 2008). For the AGPS, the average flux estimate decreased  
10 and the noise in the dataset increased with increasing closure time. It is a well-known  
11 phenomenon that even a perfectly designed non-steady-state chamber will show increasing flux  
12 underestimation with increasing closure time due to the chamber's feedback on the soil gas  
13 concentration profile if it is not corrected for in the flux calculation (Creelman et al., 2013).  
14 Regarding the increasing noise level, Koskinen et al. (2014) reported for their automated  
15 chamber system that the SR flux curves became erratic in several cases after a closure time of  
16 more than 300 s; this might have been related to wind gusts or  $\text{CO}_2$  saturation effects.

### 17 **4.3 Effect of data processing on flux rates**

18 Based on Fick's first law of diffusion, the GHG flux rate should decline with increasing  
19 chamber deployment time due to a decreasing diffusion gradient between the air-filled soil pore  
20 space and the chamber headspace (Davidson et al., 2002). Thus theoretically, gas concentration  
21 curves obtained by non-steady-state chambers are always nonlinear. However, whether  
22 nonlinearity can be detected with sufficient statistical significance depends on the length of the  
23 measurement time, the number of sampling points during the measurement, and the precision  
24 of the gas concentration measurement (Kutzbach et al., 2007; Pedersen et al., 2010). As a  
25 consequence of the high noise in the AGPS flux dataset, the majority of the flux measurements  
26 were best-fitted linearly whereas most of the LI-8100A fluxes were best-fitted nonlinearly.  
27 However, the use of a linear fit may result in a significant underestimation of the flux by at least  
28 a few percent in most soils (Davidson et al., 2002; Kutzbach et al., 2007; Pedersen et al., 2010).  
29 Creelman et al. (2013) have demonstrated in a model simulation that an exponential fit yields  
30 much better results over a wide range of soil types and air diffusivities. A linear fit only seems  
31 to be suitable for soils with a low diffusivity or for measurements with a closure time of less  
32 than 3 min (Jassal et al., 2012; Creelman et al., 2013). This evidence suggests again that the

1 discrepancies observed between the AGPS and the LI-8100A flux dataset are to a large extent  
2 caused by CO<sub>2</sub> flux underestimation of the AGPS.

3 Over the last years, several advanced nonlinear flux models based on diffusion theory have  
4 been developed (Kutzbach et al., 2007; Pedersen et al., 2010; Venterea, 2013). The HMR model  
5 selected for the AGPS dataset accounts for lateral diffusion losses and chamber leakages  
6 (Pedersen et al., 2010; Venterea, 2013). Therefore, it appeared to be well suited for the flux  
7 calculation since the detection and subsequent discarding of leaky measurements still presents  
8 the biggest challenge for the processing of automated chamber datasets. In a study on N<sub>2</sub>O  
9 fluxes, the HMR-based flux estimates were indeed less sensitive to chamber leakages and lateral  
10 diffusion than other advanced nonlinear flux models, but the model also constantly showed the  
11 highest flux underestimation across a wide range of environmental conditions (Venterea, 2013).  
12 However, the study was based on model simulations with only five sampling points during the  
13 chamber closure time. It still has to be tested if this underestimation also prevails when fitting  
14 the HMR model with high temporal frequency data. A general problem of all nonlinear models  
15 is that they are very sensitive to noise at the beginning of the chamber deployment time resulting  
16 either in flux over- or underestimation. To avoid this problem, the deadband has been  
17 introduced in the flux calculation procedure, but this initial data discarding leads to inherent  
18 flux underestimation (Kutzbach et al., 2007; Forbrich et al., 2010). Thus, flux biases due to the  
19 flux calculation method cannot be ruled out for both automated chamber systems, but these  
20 biases can only be accurately quantified under laboratory conditions (Pihlatie et al., 2013) or  
21 with advanced model simulations (Creelman et al., 2013).

22 Besides the flux calculation, the other important data processing step is the flux quality control.  
23 Currently, there are no standardized procedures available for checking the quality of chamber  
24 flux datasets like they are in the eddy covariance community (Vargas et al., 2011). The  
25 challenge is to find criteria which are able to identify faulty measurements of different origins,  
26 but at the same time not to discard large amounts of good flux measurements as well. The  
27 RMSE seems to be such a promising criterion (Christiansen et al., 2011; Jassal et al., 2012;  
28 Görres et al., 2014). Since the susceptibility of the chamber methodology to certain  
29 measurement artefacts changes with environmental conditions, any filtering can lead to a bias  
30 in the temporal resolution of the flux dataset and thus change the conclusions of field  
31 measurements. In the present study, this was very obvious for the AGPS dataset. For the LI-  
32 8100A, the filtering also introduced a temporal bias since the chambers were most susceptible

1 to headspace temperature changes and thus most of the data were discarded during the open  
2 canopy phase. However, the amount of data collectible with the LI-8100A was so high that  
3 even a discard of a quarter of the data did not alter the modelled SR balance significantly.  
4 Comparing the unfiltered and filtered dataset should be the last step of any flux quality control  
5 protocol as it can give valuable insights into the performance of the chambers and potential  
6 measurement artefacts, but it also offers a way to check the quality of the filter protocol itself.

#### 7 **4.4 Nighttime chamber measurements**

8 Obtaining reliable nighttime SR fluxes is one of the biggest remaining methodological  
9 challenges. During nighttime, atmospheric turbulences tend to calm down. Consequently, CO<sub>2</sub>  
10 diffusing out of the soil is not transported away anymore from the emission site, but starts to  
11 accumulate on the soil surface leading to a very steep CO<sub>2</sub> gradient between 0 and 100 cm  
12 above the soil surface (Schneider et al., 2009; Lai et al., 2012). However, the accumulation of  
13 CO<sub>2</sub> on the soil surface leads to a decreasing CO<sub>2</sub> gradient between the soil pore space and the  
14 atmosphere, and thus a decreasing diffusive flux. In case of manual chamber measurements,  
15 any atmospheric layering is already inevitably disturbed by the presence of the chamber  
16 operator and subsequently by the chamber deployment itself. This leads first to a flush of CO<sub>2</sub>  
17 into the chamber during chamber placement when the CO<sub>2</sub> layer directly above the soil surface  
18 is broken up, and secondly to an increasing soil-atmosphere CO<sub>2</sub> gradient (Schneider et al.,  
19 2009; Lai et al., 2012; Koskinen et al., 2014). Both effects result in a flux overestimation, and  
20 Schneider et al. (2009) have questioned if it is at all possible to obtain reliable nighttime fluxes  
21 with chambers under calm conditions.

22 This is a serious problem since nighttime chamber measurements have been used to assess the  
23 measurement bias of the eddy covariance method which systematically underestimates CO<sub>2</sub>  
24 fluxes during calm night conditions (Baldocchi, 2003; Schneider et al., 2009). Solutions to  
25 obtain unbiased nighttime flux estimates have focused thus far on the chamber deployment  
26 time, on empirical methods to correct biased flux measurements or on the use of daytime  
27 respiration data instead (Schneider et al., 2009; Lai et al., 2012; Koskinen et al., 2014). We  
28 argue that automated chambers have the potential to provide reliable nighttime flux datasets if  
29 they fulfil certain design criteria regarding chamber height, direction of chamber movement,  
30 chamber closing speed, and sample inlet position. The combination of a low chamber height  
31 (<20 cm) and a mainly horizontal movement of the chamber from its parking position to the  
32 collar increases the probability that the chamber stays within a stable atmospheric layer which

1 has no steep vertical CO<sub>2</sub> gradient. A gentle chamber movement during the closing procedure  
2 reduces the risk of breaking up that stable atmospheric layer and to mix it with overlaying  
3 atmospheric layers which have lower CO<sub>2</sub> concentrations. Regarding the position of the sample  
4 inlet, the AGPS is to our knowledge the only automated chamber system which has the inlet  
5 inside the collar instead of the chamber. This offered the unique opportunity to measure the  
6 undisturbed atmospheric CO<sub>2</sub> concentration 5 cm above the soil surface before the chamber  
7 moved over the collar. About 17 % of the AGPS measurements showed a decrease in the CO<sub>2</sub>  
8 headspace concentration during the 1 min deadband. The open AGPS chamber which was not  
9 flushed before the closure and which was parked about 10 cm above the soil surface, probably  
10 had a lower CO<sub>2</sub> concentration inside than the atmospheric layer less than 10 cm above the soil  
11 surface. Closing the chamber and starting the sample air flow broke up the atmospheric  
12 layering, mixed the two air layers and led to a dilution of the CO<sub>2</sub> headspace concentration.  
13 This dilution is equivalent to the initial CO<sub>2</sub> flush into the chamber observed by Koskinen et al.  
14 (2014) who measured the pre-closure CO<sub>2</sub> concentration inside the chamber. Thus, the unique  
15 design of the AGPS offers the possibility to directly detect for each measurement plot artificial  
16 increases in the soil-atmosphere CO<sub>2</sub> gradient in calm nights and filter out obviously disturbed  
17 flux measurements. Moreover, the AGPS measurements have shown that this chamber artefact  
18 is indeed mainly a nighttime problem, but it might also affect part of the daytime flux  
19 measurements.

20 The design of the LI-8100A chambers with the sample inlet and outlet positioned inside the  
21 chamber did not allow to detect any dilution of the atmospheric CO<sub>2</sub> concentration because no  
22 undisturbed pre-closure CO<sub>2</sub> concentration measurement directly above the collar was  
23 available. The chamber headspace was already mixed before the chamber closure. It is therefore  
24 not possible to say if part of the LI-8100A nighttime measurements at high ambient CO<sub>2</sub>  
25 concentrations have been overestimated.

26

## 27 **5 Recommendations for automation of soil respiration measurements**

28 The closed dynamic chamber method is an invasive method and biases in soil GHG flux  
29 estimates can be introduced by environmental alterations due to the presence of the chamber,  
30 alterations of the chamber performance due to changes in environmental conditions, as well as  
31 the data processing. Environmental alterations due to the presence of the chamber are a serious  
32 concern for automated chamber systems, with the probability of environmental alterations



1 increasing with the size of the chamber structure. It is therefore recommended to regularly move  
2 automated chambers between different permanently installed collars to prevent any significant  
3 chamber-induced changes for example in soil moisture. However, depending on the ecosystem  
4 and the collar insertion depth, this recommendation should not be limited to the aboveground  
5 part of the chamber. We showed that collars can restrict horizontal root growth leading to the  
6 formation of roots mat along the inside collar walls and thus potentially to artificially increased  
7 SR.

8 Selecting the most appropriate collar insertion depth for a specific study site is always a trade-  
9 off between reducing the collar impact on the root system and preventing lateral soil gas  
10 diffusion during measurements. Lateral soil gas diffusion due to insufficient collar insertion  
11 depth is one of the major causes of significant soil GHG flux underestimation, and also one of  
12 the processes most affected by changes in environmental conditions as it increases with  
13 increasing air-filled soil pore space. Flux underestimation due to leakages in the chamber  
14 system can be reduced by shortening the chamber deployment time and by choosing the  
15 appropriate flux calculation model. Shortening the deployment time is no longer a problem with  
16 the available field deployable gas analysers which are able to measure at 1 Hz frequency.  
17 Regarding the flux calculation, several advanced nonlinear flux calculation models have been  
18 developed in recent years, but none of them seems to be able to fully correct flux estimates for  
19 leakages. However, the models have mainly been tested against data from manual chambers  
20 with only few sample points per measurement.

21 Accounting for leakages and other measurement artefacts in unsupervised operating automated  
22 chamber systems is still a big challenge. Currently, no standardized protocols exist for checking  
23 the quality of automated chamber flux datasets. We propose to include a comparison of the  
24 unfiltered and filtered dataset in any flux quality control protocol. Such a comparison can give  
25 valuable insights into the performance of automated chamber systems under different  
26 environmental conditions and reveal chamber-induced measurement artefacts, but it also offers  
27 a way to check the quality of the filter protocol itself. Based on the design of one of the  
28 automated chamber systems which had the sample inlet inside the collar instead of the chamber,  
29 we included a filter criterion based on the headspace CO<sub>2</sub> concentration change during the  
30 deadband period. The combination of this unique chamber design feature and the filter criterion  
31 offered the possibility to detect disturbed chamber measurements during nights with a stratified  
32 atmosphere. Obtaining unbiased nighttime respiration measurements is a major challenge

1 which has not been resolved yet. We showed for the first time that automated chamber systems  
2 have the potential to solve this issue if certain design criteria are considered. Thus besides  
3 providing high temporal frequency flux data, automated chamber systems would offer another  
4 possibility to greatly improve our understanding of soil GHG fluxes.

5

## 6 **Acknowledgements**

7 The authors thank Nicola Arriga, Joris Cools, Fred Kockelbergh, Kristof Mouton, Jan Segers,  
8 UIT, Stefan Vanbeveren, and Marc Wellens for their technical assistance at the field site. We  
9 also acknowledge Gerald Moser (Justus Liebig University Giessen, Germany) who analyzed  
10 the soil CO<sub>2</sub> samples, as well as Anne Cools (University of Antwerp, Belgium) for performing  
11 the DOC analysis. Funding for this research was provided by ERC Advanced Grant agreement  
12 (# 233366) POPFULL under the EC 7<sup>th</sup> Framework Programme (FP7/2007-2013), the  
13 Flemish Hercules Foundation as Infrastructure contract # ZW09-06, and the Methusalem  
14 Program of the Flemish Government.

15

## 16 **References**

- 17 Ambus, P., Skiba, U., Drewer, J., Jones, S. K., Carter, M. S., Albert, K. R., and Sutton, M. A.:  
18 Development of an accumulation-based system for cost-effective chamber measurements of  
19 inert trace gas fluxes, *Eur J Soil Sci*, 61, 785–792, 2010.
- 20 Bain, W. G., Hutrya, L., Patterson, D. C., Bright, A. V., Daube, B. C., Munger, J. W., and  
21 Wofsy, S. C.: Wind-induced error in the measurement of soil respiration using closed dynamic  
22 chambers, *Agr Forest Meteorol*, 131, 225–232, 2005.
- 23 Baldocchi, D. D.: Assessing the eddy covariance technique for evaluating carbon dioxide  
24 exchange rates of ecosystems: past, present and future, *Glob Change Biol*, 9, 479–492, 2003.
- 25 Berhongaray, G., Verlinden, M. S., Broeckx, L. S., and Ceulemans, R.: Changes in  
26 belowground biomass after coppice in two *Populus* genotypes, *Forest Ecol Manag*, 337, 1–10,  
27 2015.
- 28 Breuer, L., Papen, H., and Butterbach-Bahl, K.: N<sub>2</sub>O emission from tropical forest soils of  
29 Australia, *J. Geophys. Res*, 105, 26353–26367, 2000.

- 1 Broeckx, L. S., Verlinden, M. S., and Ceulemans, R.: Establishment and two-year growth of a  
2 bio-energy plantation with fast-growing *Populus* trees in Flanders (Belgium): Effects of  
3 genotype and former land use, *Biomass Bioenerg*, 42, 151–163, 2012.
- 4 Brummell, M. E. and Siciliano, S. D.: Measurement of carbon dioxide, methane, nitrous oxide,  
5 and water potential in soil ecosystems, *Method Enzymol*, 496, 115–137, 2011.
- 6 Carbone, M. S. and Vargas, R.: Automated soil respiration measurements: new information,  
7 opportunities and challenges, *New Phytol*, 177, 295–297, 2008.
- 8 Christiansen, J., Korhonen, J. J., Juszczak, R., Giebels, M., and Pihlatie, M.: Assessing the  
9 effects of chamber placement, manual sampling and headspace mixing on CH<sub>4</sub> fluxes in a  
10 laboratory experiment, *Plant Soil*, 343, 171-185, 2011.
- 11 Collier, S. M., Ruark, M. D., Oates, L. G., Jokela, W. E., and Dell, C. J.: Measurement of  
12 greenhouse gas flux from agricultural soils using static chambers, *J Vis Exp*, 90, e52110, 2014.
- 13 Creelman, C., Nickerson, N., and Risk, D.: Quantifying lateral diffusion error in soil carbon  
14 dioxide respiration estimates using numerical modeling, *Soil Sci Soc Am J*, 77, 699–708, 2013.
- 15 Davidson, E. A., Savage, K., Verchot, L. V., and Navarro, R.: Minimizing artifacts and biases  
16 in chamber-based measurements of soil respiration, *Agr Forest Meteorol*, 113, 21–37, 2002.
- 17 de Klein, C., and Harvey, M. (eds.): Nitrous oxide chamber methodology guidelines, Ministry  
18 for Primary Industries, New Zealand, online available at:  
19 [http://www.globalresearchalliance.org/research/livestock/activities/nitrous-oxide-chamber-  
20 methodology-guidelines/](http://www.globalresearchalliance.org/research/livestock/activities/nitrous-oxide-chamber-<br/>20 methodology-guidelines/), 2012.
- 21 Denmead, O. T.: Chamber systems for measuring nitrous oxide emission from soils in the field,  
22 *Soil Sci Soc Am J*, 43, 89–95, 1979.
- 23 FAO: Agriculture, forestry and other land use emissions by sources and removals by sinks:  
24 1990 - 2011 analysis. FAO Statistics Division Working Paper Series, Rome, 2014.
- 25 Forbrich, I., Kutzbach, L., Hormann, A., and Wilmking, M.: A comparison of linear and  
26 exponential regression for estimating diffusive CH<sub>4</sub> fluxes by closed-chambers in peatlands,  
27 *Soil Biol Biochem*, 42, 507–515, 2010.
- 28 Giltrap, D. L., Li, C., and Saggar, S.: DNDC: A process-based model of greenhouse gas fluxes  
29 from agricultural soils, *Agr Ecosyst Environ*, 136, 292–300, 2010.

- 1 Görres, C.-M., Kutzbach, L., and Elsgaard, L.: Comparative modeling of annual CO<sub>2</sub> flux of  
2 temperate peat soils under permanent grassland management, *Agr Ecosyst Environ*, 186, 64–  
3 76, 2014.
- 4 Hashimoto, S., and Komatsu, H.: Relationships between soil CO<sub>2</sub> concentration and CO<sub>2</sub>  
5 production, temperature, water content, and gas diffusivity: implications for field studies  
6 through sensitivity analyses, *J For Res*, 11, 41–50, 2006.
- 7 Heinemeyer, A., Di Bene, C., Lloyd, A. R., Tortorella, D., Baxter, R., Huntley, B., Gelsomino,  
8 A., and Ineson, P.: Soil respiration: implications of the plant-soil continuum and respiration  
9 chamber collar-insertion depth on measurement and modelling of soil CO<sub>2</sub> efflux rates in three  
10 ecosystems, *Eur J Soil Sci*, 62, 82–94, 2011.
- 11 Heinemeyer, A. and McNamara, N. P.: Comparing the closed static versus the closed dynamic  
12 chamber flux methodology: Implications for soil respiration studies, *Plant Soil*, 346, 145–151,  
13 2011.
- 14 Hopkins, F., Gonzalez-Meler, M. A., Flower, C. E., Lynch, D. J., Czimczik, C., Tang, J., and  
15 Subke, J.-A.: Ecosystem-level controls on root-rhizosphere respiration. *New Phytol*, 199, 339–  
16 351, 2013.
- 17 Huber, P.: *Robust Statistics*, Wiley, New York, USA, 1981.
- 18 Hutchinson, G. L. and Livingston, G. P.: Vents and seals in non-steady-state chambers used for  
19 measuring gas exchange between soil and the atmosphere, *Eur J Soil Sci*, 52, 675–682, 2001.
- 20 Janssens, I. A., Kowalski, A. S., Longdoz, B., and Ceulemans, R.: Assessing forest soil CO<sub>2</sub>  
21 efflux: an in situ comparison of four techniques, *Tree Physiol*, 20, 23–32, 2000.
- 22 Jassal, R., Black, A., Novak, M., Morgenstern, K., Nestic, Z., and Gaumont-Guay, D.:  
23 Relationship between soil CO<sub>2</sub> concentrations and forest-floor CO<sub>2</sub> effluxes, *Agr Forest*  
24 *Meteorol*, 130, 176–192, 2005.
- 25 Jassal, R. S., Black, T. A., Nestic, Z., and Gaumont-Guay, D.: Using automated non-steady-state  
26 chamber systems for making continuous long-term measurements of soil CO<sub>2</sub> efflux in forest  
27 ecosystems, *Agr Forest Meteorol*, 161, 57–65, 2012.
- 28 Jones, H. G.: *Plants and microclimate: A quantitative approach to environmental plant*  
29 *physiology*, Cambridge University Press, Cambridge, UK, 1992.

1 Kitzler, B., Zechmeister-Boltenstern, S., Holtermann, C., Skiba, U., and Butterbach-Bahl, K.:  
2 Nitrogen oxides emission from two beech forests subjected to different nitrogen loads,  
3 *Biogeosciences*, 3, 293–310, 2006.

4 Koskinen, M., Minkkinen, K., Ojanen, P., Kämäräinen, M., Laurila, T., and Lohila, A.:  
5 Measurements of CO<sub>2</sub> exchange with an automated chamber system throughout the year:  
6 challenges in measuring night-time respiration on porous peat soil, *Biogeosciences*, 11, 347–  
7 363, 2014.

8 Kutzbach, L., Schneider, J., Sachs, T., Giebels, M., Nykänen, H., Shurpali, N. J., Martikainen,  
9 P. J., Alm, J., and Wilmking, M.: CO<sub>2</sub> flux determination by closed-chamber methods can be  
10 seriously biased by inappropriate application of linear regression, *Biogeosciences*, 4, 1005–  
11 1025, 2007.

12 Lai, D. Y. F., Roulet, N. T., Humphreys, E. R., Moore, T. R., and Dalva, M.: The effect of  
13 atmospheric turbulence and chamber deployment period on autochamber CO<sub>2</sub> and CH<sub>4</sub> flux  
14 measurements in an ombotrophic peatland, *Biogeosciences*, 9, 3305–3322, 2012.

15 Levy, P. E., Gray, A., Leeson, S. R., Gaiawyn, J., Kelly, M. P. C., Cooper, M. D. A., Dinsmore,  
16 K. J., Jones, S. K., and Sheppard, L. J.: Quantification of uncertainty in trace gas fluxes  
17 measured by the static chamber method, *Eur J Soil Sci*, 62, 811–821, 2011.

18 LI-COR Biosciences: LI-8100A Automated Soil CO<sub>2</sub> Flux System & LI-8150 Multiplexer  
19 Instruction Manual, online available at: [http://envsupport.licor.com/docs/LI-](http://envsupport.licor.com/docs/LI-8100A_Manual.pdf)  
20 [8100A\\_Manual.pdf](http://envsupport.licor.com/docs/LI-8100A_Manual.pdf), 2010.

21 Liu, G. and Si, B. C.: Multi-layer diffusion model and error analysis applied to chamber-based  
22 gas fluxes measurements, *Agr Forest Meteorol*, 149, 169–178, 2009.

23 Lloyd, J. and Taylor, J. A.: On the temperature dependence of soil respiration, *Funct Ecol*, 8,  
24 315–323, 1994.

25 Maier, M. and Schack-Kirchner, H.: Using the gradient method to determine soil gas flux: A  
26 review, *Agr Forest Meteorol*, 192–193, 78–95, 2014.

27 Millington, R. J. and Quirk, J. P.: Permeability of porous solids, *Trans. Faraday Soc.*, 57, 1200–  
28 1207, 1961.

29 Olander, L. P., Wollenberg, E., Tubiello, F. N., and Herold, M.: Synthesis and Review:  
30 Advancing agricultural greenhouse gas quantification, *Environ Res Lett*, 9, 75003, 2014.

1 Parkin, T., and Venterea, R.: Chapter 3. Chamber-based trace gas flux measurements, in: Follet,  
2 R. (ed.): Sampling Protocols, pp. 3-1 to 3-39, online available at:  
3 [www.ars.usda.gov/research/GRACEnet](http://www.ars.usda.gov/research/GRACEnet), 2010.

4 Pedersen, A. R., Petersen, S. O., and Schelde, K.: A comprehensive approach to soil-  
5 atmosphere trace-gas flux estimation with static chambers, *Eur J Soil Sci*, 61, 888–902, 2010.

6 Peltola, O., Mammarella, I., Haapanala, S., Burba, G., and Vesala, T.: Field intercomparison of  
7 four methane gas analyzers suitable for eddy covariance flux measurements, *Biogeosciences*,  
8 10, 3749–3765, 2013.

9 Petersen, S.O.: Diffusion probe for gas sampling in undisturbed soil, *Eur J Soil Sci*, 65, 663–  
10 671, 2014.

11 Phillips, R., Griffith, D. W., Dijkstra, F., Lugg, G., Lawrie, R., and Macdonald, B.: Tracking  
12 short-term effects of nitrogen-15 addition on nitrous oxide fluxes using fourier-transform  
13 infrared spectroscopy, *J Environ Qual*, 42, 1327–1340, 2013.

14 Pihlatie, M. K., Christiansen, J. R., Aaltonen, H., Korhonen, J. F. J., Nordbo, A., Rasilo, T.,  
15 Benanti, G., Giebels, M., Helmy, M., Sheehy, J., Jones, S., Juszczak, R., Klefoth, R., Lobo-do-  
16 Vale, R., Rosa, A. P., Schreiber, P., Serça, D., Vicca, S., Wolf, B., and Pumpanen, J.:  
17 Comparison of static chambers to measure CH<sub>4</sub> emissions from soils, *Agr Forest Meteorol*,  
18 171–172, 124–136, 2013.

19 Pumpanen, J., Kolari, P., Ilvesniemi, H., Minkkinen, K., Vesala, T., Niinistö, S., Lohila, A.,  
20 Larmola, T., Morero, M., Pihlatie, M., Janssens, I., Yuste, J. C., Grünzweig, J. M., Reth, S.,  
21 Subke, J.-A., Savage, K., Kutsch, W., Østreng, G., Ziegler, W., Anthoni, P., Lindroth, A., and  
22 Hari, P.: Comparison of different chamber techniques for measuring soil CO<sub>2</sub> efflux, *Agr Forest*  
23 *Meteorol*, 123, 159–176, 2004.

24 Qu, W., Bogaen, H. R., Huisman, J. A., and Vereecken, H.: Calibration of a novel low-cost soil  
25 water content sensor based on a ring oscillator, *Vadose Zone J*, 12, 1–10, 2013.

26 R Core Team: R: A language and environment for statistical computing. R Foundation for  
27 Statistical Computing, Vienna, Austria, 2014.

28 Roland, M., Vicca, S., Bahn, M., Ladreiter-Knauss, T., Schmitt, M., and Janssens, I. A.:  
29 Importance of nondiffusive transport for soil CO<sub>2</sub> efflux in a temperate mountain grassland, *J.*  
30 *Geophys. Res. Biogeosci.*, 120, 502–512, 2015.

1 Rühlmann, J., Körschens, M., and Graefe, J.: A new approach to calculate the particle density  
2 of soils considering properties of the soil organic matter and the mineral matrix, *Geoderma*,  
3 130, 272–283, 2006.

4 Ryan, J. A., and Ulrich, J. M.: xts: eXtensible Time Series: R package version 0.9-7, online  
5 available at: <http://CRAN.R-project.org/package=xts>, 2014.

6 Savage, K., Phillips, R., and Davidson, E.: High temporal frequency measurements of  
7 greenhouse gas emissions from soils, *Biogeosciences*, 11, 2709–2720, 2014.

8 Schipper, L. A., Hobbs, J. K., Rutledge, S., and Arcus, V. L.: Thermodynamic theory explains  
9 the temperature optima of soil microbial processes and high Q10 values at low temperatures,  
10 *Glob Change Biol*, 20, 3578–3586, 2014.

11 Schneider, J., Kutzbach, L., Schulz, S., and Wilmking, M.: Overestimation of CO<sub>2</sub> respiration  
12 fluxes by the closed chamber method in low-turbulence nighttime conditions, *J. Geophys. Res.*,  
13 114, G03005, 2009.

14 Turcu, V. E., Jones, S. B., and Or, D.: Continuous soil carbon dioxide and oxygen  
15 measurements and estimation of gradient-based gaseous flux, *Vadose Zone J*, 4, 1161–1169,  
16 2005.

17 van Rij, J., Wieling, M., Baayen, R., and van Rijn, H.: itsadug: Interpreting Time Series and  
18 Autocorrelated Data Using GAMMs, R package version 1.0.1, 2015.

19 Vargas, R., Carbone, M., Reichstein, M., and Baldocchi, D.: Frontiers and challenges in soil  
20 respiration research: from measurements to model-data integration, *Biogeochemistry*, 102, 1–  
21 13, 2011.

22 Venterea, R. T.: Theoretical comparison of advanced methods for calculating nitrous oxide  
23 fluxes using non-steady state chambers, *Soil Sci Soc Am J*, 77, 709–720, 2013.

24 Venterea, R.T., Baker, J. M.: Effects of soil physical nonuniformity on chamber-based gas flux  
25 estimates, *Soil Sci Soc Am J*, 72, 1410–1417, 2008.

26 Venterea, R. T., Spokas, K. A., and Baker, J. M.: Accuracy and precision analysis of chamber-  
27 based nitrous oxide gas flux estimates, *Soil Sci Soc Am J*, 73, 1087–1093, 2008.

28 Verlinden, M. S., Broeckx, L. S., Wei, H., and Ceulemans, R.: Soil CO<sub>2</sub> efflux in a bioenergy  
29 plantation with fast-growing *Populus* trees – influence of former land use, inter-row spacing  
30 and genotype, *Plant Soil*, 369, 631–644, 2013.

- 1 Wang, K., Liu, C., Zheng, X., Pihlatie, M., Li, B., Haapanala, S., Vesala, T., Liu, H., Wang, Y.,  
2 Liu, G., and Hu, F.: Comparison between eddy covariance and automatic chamber techniques  
3 for measuring net ecosystem exchange of carbon dioxide in cotton and wheat fields,  
4 *Biogeosciences*, 10, 6865–6877, 2013.
- 5 Weylandt, M. R.: xtsExtra: Supplementary Functionality for xts: R package version 0.0-1/r824,  
6 online available at: <http://R-Forge.R-project.org/projects/xts/>, 2014.
- 7 Wood, S. N.: *Generalized Additive Models: An Introduction with R*, Chapman and Hall/CRC,  
8 2006.
- 9 Xu, L., Furtaw, M. D., Madsen, R. A., Garcia, R. L., Anderson, D. J., and McDermitt, D. K.:  
10 On maintaining pressure equilibrium between a soil CO<sub>2</sub> flux chamber and the ambient air, *J.*  
11 *Geophys. Res.*, 111, D08S10, 2006.
- 12 Zeileis, A. and Grothendieck, G.: zoo: S3 infrastructure for regular and irregular time series, *J*  
13 *Stat Softw*, 14, 1–27, 2005.
- 14 Zenone, T., Zona, D., Gelfand, I., Gielen, B., Camino-Serrano, M., and Ceulemans, R.: CO<sub>2</sub>  
15 uptake is offset by CH<sub>4</sub> and N<sub>2</sub>O emissions in a poplar short rotation coppice, *Glob Change*  
16 *Biol Bioenerg*, doi: 10.1111/gcbb.12269, 2015.
- 17 Zhou, W., Hui, D., and Shen, W.: Effects of soil moisture on the temperature sensitivity of soil  
18 heterotrophic respiration: a laboratory incubation study, *PloS ONE*, 9, e92531, 2014.
- 19



1 Table 1. Technical specifications of the two tested automated chamber systems.

		<b>Greenhouse Gas Monitoring System AGPS</b>	<b>LI-8100A Automated Soil CO<sub>2</sub> Flux System</b>
<b>Chamber</b>	Dimensions <sup>a</sup>	200 cm L x 80 cm W x 50 cm H	48 cm L x 38 cm W x 33 cm H
	Headspace volume	25000 cm <sup>3</sup> , square	4076 cm <sup>3</sup> , round
	Material	stainless steel frame with white FOREX box	white coated stainless steel
	Sealing	1 continuous hollow and soft PVC strip per chamber side, 1 cm thick, transparent	1 neoprene gasket plus 1 neoprene collar gasket, black
	Vent	20 cm long tube on the outside, 1 cm I.D. <sup>b</sup>	special vent design <sup>c</sup>
	Fan	no	no
<b>Collar</b>	Dimensions	48 cm x 48 cm <sup>d</sup> /58 cm x 58 cm <sup>e</sup>	20.3 cm I.D./21.3 cm O.D.
	Enclosed soil area	2304 cm <sup>2</sup>	318 cm <sup>2</sup>
	Insertion depth	~ 3 cm	~ 7 cm
	Offset <sup>f</sup>	2.1±0.7 cm	4.1±1.1 cm
	Material	stainless steel	PVC, green
<b>Tubing<sup>g</sup></b>	Length	11 – 25 m	15 m
	Diameter	6.0 mm I.D.	3.2 mm I.D.
	Material	PTFE, protected inside a black plastic tube	Bev-a-line, protected inside a black plastic tube
<b>Flow rate</b>		3.0-3.2 lpm <sup>g</sup> /0.4-0.5 lpm <sup>h</sup>	2.4-2.9 lpm <sup>g</sup> /1.7 lpm <sup>h</sup>
<b>Multiplexer pump</b>		diaphragm	diaphragm
<b>Gas analyser</b>	Principle	Off-Axis Integrated Cavity Output Spectroscopy	Non-dispersive Infrared
	Measurement range	200-4000 ppm <sup>i</sup> , 7000-70000 ppm <sup>i</sup>	0-20000 ppm <sup>i</sup> , 0-40 mmol/mol <sup>j</sup>
	Uncertainty	total uncertainty: <0.25 % of reading <sup>i,j,m</sup> precision <sup>n</sup> CO <sub>2</sub> : 150 ppb precision <sup>n</sup> H <sub>2</sub> O: 100 ppm	accuracy: 1.5 % of reading <sup>i,j</sup> RMS noise CO <sub>2</sub> : <1 ppm <sup>k</sup> RMS noise H <sub>2</sub> O: <0.01 mmol/mol <sup>l</sup>
	<b>Total gas volume</b>		30294-33719 cm <sup>3</sup>
<b>Operational range</b>	Chamber	>2 °C, RH: non-condensing <sup>o</sup>	-20 to 45 °C, 0 to 95 % RH (non-condensing)
	Gas analyser	0 to 45 °C, <98 % RH (non-condensing)	-20 to 45 °C, 0 to 95 % RH (non-condensing)
<b>Accessories</b>	Air temperature	Easytemp TMR31, Pt100 A	thermistor, accuracy ±0.5 °C
	Soil temperature	SPADE <sup>p</sup> , DS18B20 digital thermometer, accuracy ±0.5 °C	thermistor, accuracy ±1.0 °C
	Soil moisture	SPADE <sup>p</sup> , ring oscillator, relative accuracy ±4 %	Decagon ECH <sub>2</sub> O model EC-5, ±3% VWC, most mineral soils
	Air pressure	not implemented	1.5 % accuracy
<b>Power requirement</b>		max. 2000 W	max. 60 W

<sup>a</sup> the entire supporting structure, not only the chamber itself, <sup>b</sup> according to Parkin and Venterea (2010); unlike the LI-8100A vent, this one was not specifically tested, <sup>c</sup> Xu et al. (2006) <sup>d</sup> internal, <sup>e</sup> rim included, <sup>f</sup> collar height above the soil surface, <sup>g</sup> chamber to multiplexer, <sup>h</sup> multiplexer to gas analyser, <sup>i</sup> CO<sub>2</sub>, <sup>j</sup> H<sub>2</sub>O, <sup>k</sup> at 370 ppm with 1 s signal averaging, <sup>l</sup> at 10 ppt with 1 s signal averaging, <sup>m</sup> without calibration, <sup>n</sup> 1-sigma, 5 s signal averaging, <sup>o</sup> incorporated

---

freeze protection which automatically puts the system into standby when ambient air temperature drops below 2 °C; however, the chambers could also work at lower temperatures, <sup>p</sup> the soil temperature and soil moisture sensor are incorporated into one device (Qu et al., 2013).

L: length, W: width, H: height, RH: relative humidity. I.D.: inner diameter, O.D.: outer diameter.

1

2

1 Table 2. Number of discarded CO<sub>2</sub> fluxes after each filter step for the two automated chamber  
2 systems (LIN = linear fit, EXP = exponential fit, SSN<sub>Lin</sub> = normalized sum of squares of  
3 residuals for linear fit,  $\Delta T_{\text{air}}$  = change in air temperature inside the closed chamber during the  
4 closure time,  $\Delta \text{CO}_2$  = difference in the atmospheric CO<sub>2</sub> concentration 5 cm above the collar  
5 directly before chamber closure and after a deadband of 1 min, RH = relative humidity, NA =  
6 information not available for that chamber system). Datasets were grouped by time of the day  
7 and stability of the atmospheric CO<sub>2</sub> concentration at 50 cm above the soil surface. Day and  
8 night were based on sun rise and sunset times. Atmospheric CO<sub>2</sub> concentration was considered  
9 as constant when the standard deviation for a 3-min measurement prior to the chamber closures  
10 was  $\leq 1.0$  ppm. The AGPS total closure time was 10 min. Fluxes were once calculated for the  
11 first 4 min of the closure time (left of the vertical line) and once for 9 min closure time (right  
12 of the vertical line), each with a 1 min deadband.

	Total		Day (constant)		Day (fluctuating)		Night (constant)		Night (fluctuating)	
	LIN	EXP	LIN	EXP	LIN	EXP	LIN	EXP	LIN	EXP
<b>AGPS</b>										
Unfiltered <sup>a</sup>	2806 4140	2105 771	580 824	492 248	1211 1780	875 306	197 276	141 62	818 1260	597 155
Negative fluxes	120 97	31 30	49 57	17 19	31 18	4 3	18 12	5 7	22 10	5 1
SSN <sub>Lin</sub> > 1.0 ppm	1717 3510	1165 719	321 699	276 223	858 1583	577 298	86 215	58 46	452 1013	254 152
-0.5 < $\Delta T_{\text{air}}$ < 1.0 °C	146 192	138 3	29 14	29 0	44 33	36 2	0 15	2 0	73 130	71 1
$\Delta \text{CO}_2 < 0.0$ ppm	88 53	58 5	8 3	8 1	30 30	20 2	14 2	1 2	36 18	29 0
RH > 100 %	NA	NA	NA	NA	NA	NA	NA	NA	NA	NA
Filtered	735 288	713 14	173 51	162 5	248 116	238 1	79 32	75 7	235 89	238 1
<b>LI-8100A</b>										
Unfiltered	5640	7233	1376	888	2781	3233	313	437	1170	2675
Negative fluxes	0	1	0	0	0	1	0	0	0	0
SSN <sub>Lin</sub> > 1.0 ppm	201	191	66	31	68	69	13	21	54	70
-0.5 < $\Delta T_{\text{air}}$ < 1.0 °C	1328	1102	533	263	663	386	11	24	121	429
$\Delta \text{CO}_2 < 0.0$ ppm	NA	NA	NA	NA	NA	NA	NA	NA	NA	NA
RH > 100 %	74	61	14	8	37	28	14	10	9	15
Filtered	4037	5878	763	586	2013	2749	275	382	986	2161

<sup>a</sup> 21 measurements discarded prior to the filtering because of missing air temperature measurements for the flux calculation

13

14

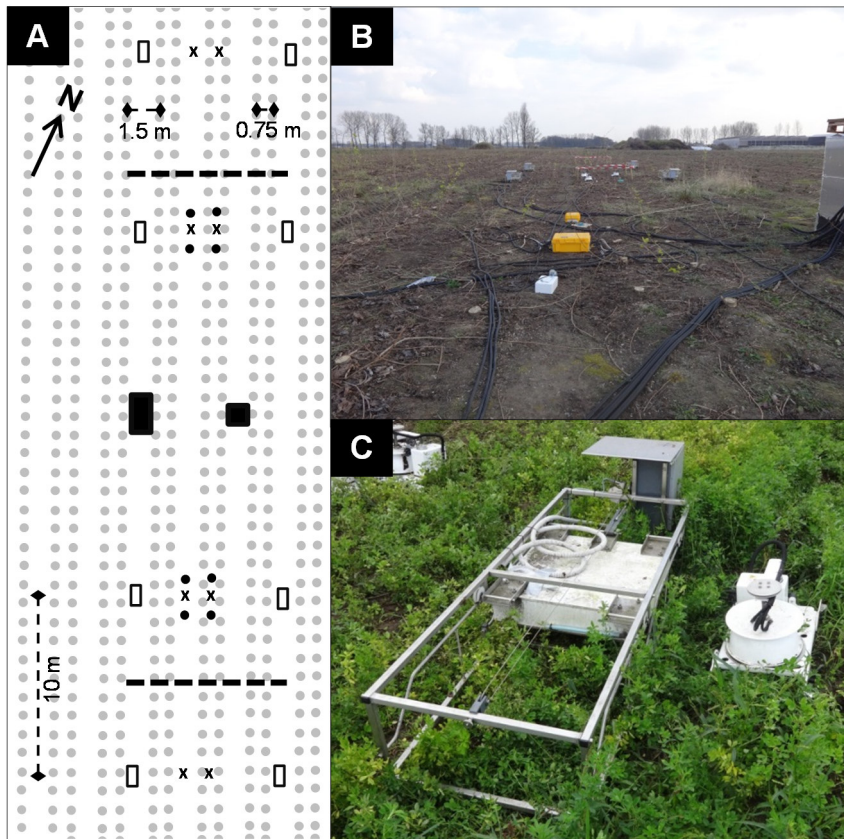
1 Table 3. Number of measurements (N), regression parameters ( $E_0$  = temperature sensitivity coefficient;  $R_{10}$  = soil respiration rate at 10 °C soil  
 2 temperature at 5 cm depth) and residual standard errors (RSE) for the Lloyd and Taylor model fits presented in Fig. 6, and cumulated average  
 3 soil respiration (cSR). Data are shown for the entire monitoring period (E, 15.04 – 31.08.2014), the open canopy phase (OC, 15.04 – 30.06.2014)  
 4 and the closed canopy phase (CC, 01.07 – 31.08.2014), respectively. The standard errors for the regression parameters and the 95 % confidence  
 5 intervals for the average cSR, respectively, are shown in brackets.

Chamber	Row type	Filtered	$N$			$E_0$			$R_{10}$			RSE			Average cSR		
			E	OC	CC	E	OC	CC	E	OC	CC	E	OC	CC	E	OC	CC
						(K)			$(\mu\text{mol CO}_2 \text{ m}^{-2} \text{ s}^{-1})$			$(\mu\text{mol CO}_2 \text{ m}^{-2} \text{ s}^{-1})$			$(\text{g CO}_2 \text{ m}^{-2})$		
AGPS	Wide	No	3378	2333	198	177	307	1.17	1.10	1.10	0.93	0.80	1.07	897	433	507	
						(10.7)	(10.9)	(28.1)	(0.03)	(0.03)	(0.07)				(838 – 956)	(409 – 458)	(449 – 567)
AGPS	Wide	Yes	1049	743	156	125	282	0.99	0.96	0.88	0.68	0.64	0.70	698	347	308	
						(18.3)	(20.1)	(53.0)	(0.04)	(0.04)	(0.10)				(655 – 742)	(327 – 367)	(334 – 430)
LI-8100A	Wide	No	4601	2367	279	222	369	1.24	1.32	1.07	0.75	0.66	0.81	1018	520	501	
						(7.5)	(8.5)	(13.6)	(0.02)	(0.02)	(0.03)				(931 – 1108)	(482 – 558)	(448 – 557)
LI-8100A	Wide	Yes	3335	1445	326	226	406	1.10	1.28	0.93	0.69	0.61	0.73	974	507	469	
						(9.5)	(13)	(14.4)	(0.02)	(0.03)	(0.03)				(878 – 1074)	(468 – 546)	(415 – 527)
LI-8100A	Narrow	No	6588	3616	230	198	263	1.77	1.77	1.76	0.87	0.80	0.91	1376	687	691	
						(5.9)	(6.8)	(10.8)	(0.02)	(0.02)	(0.04)				(1319 – 1433)	(662 – 713)	(658 – 724)

LI-8100A	Narrow	Yes	4811	2262	285	243	285	1.57	1.60	1.62	0.76	0.64	0.84	1338	668	661
					(7.0)	(9.1)	(11.2)	(0.02)	(0.03)	(0.04)				(1270 – 1406)	(638 – 699)	(627 – 695)

---

1

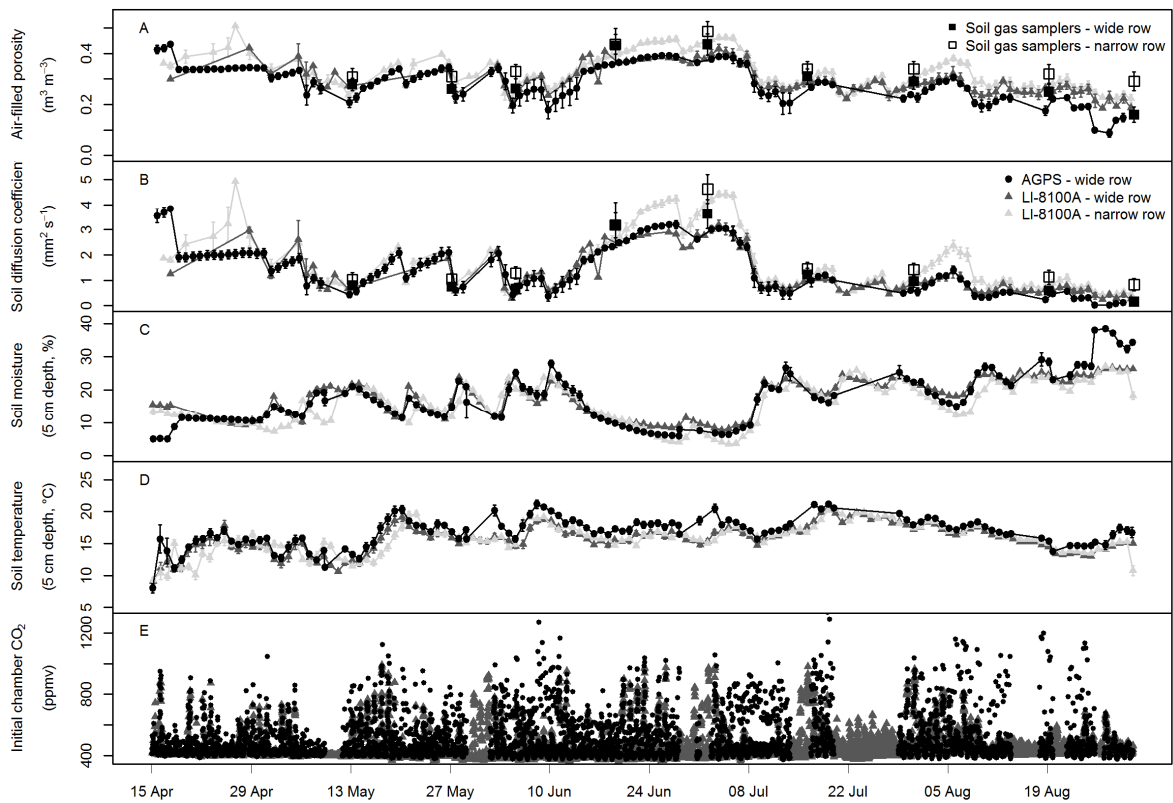


1

2 Figure 1. Schematic drawing of the field site (A), view of the southern half of the field site on  
 3 25 March 2014 shortly after the harvest (B), and size comparison of an AGPS chamber (left,  
 4 chamber open) and a LI-8100A chamber (right, chamber closed) (C). In A, the big black-filled  
 5 rectangle shows the location of the housing for the LosGatos analysers and the AGPS  
 6 multiplexer, the small black-filled rectangle the location of the LI-8100A gas analyser and  
 7 multiplexer, hollow rectangles represent AGPS chambers, black circles represent LI-8100A  
 8 chambers, crosses represent soil gas concentration measurement nests, and grey circles indicate  
 9 the position of the poplars. The dashed black lines indicate the soil sampling transects.

10

11

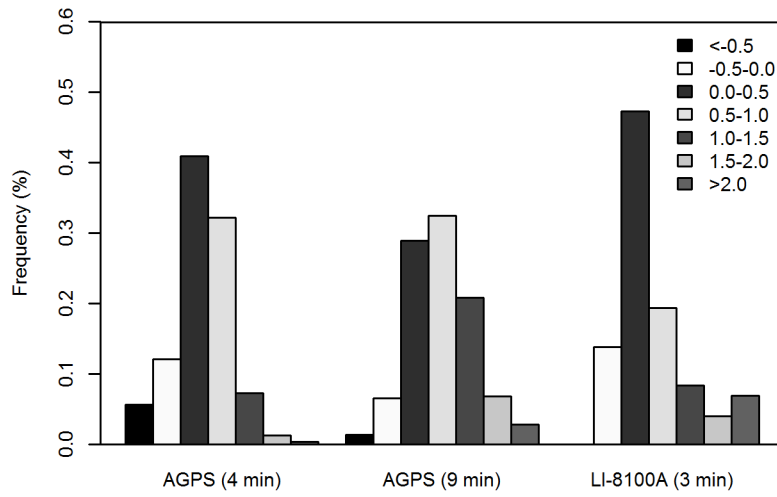


1

2 Figure 2. Comparison of different environmental variables measured by the AGPS and the LI-  
 3 8100A before each chamber closure. Panel A – D show daily averages with their respective  
 4 standard deviations. For air-filled porosity and the soil diffusion coefficient only measurements  
 5 have been included for which both soil temperature and moisture data were available from the  
 6 specific chamber at the time of the measurement. All single measurements are shown for the  
 7 initial CO<sub>2</sub> concentration (panel E) which is equivalent to the CO<sub>2</sub> concentration at time = 0 s  
 8 of the flux measurement. Measured by the AGPS prior to the chamber closure and calculated  
 9 for the LI-8100A by its internal software.

10

11



1

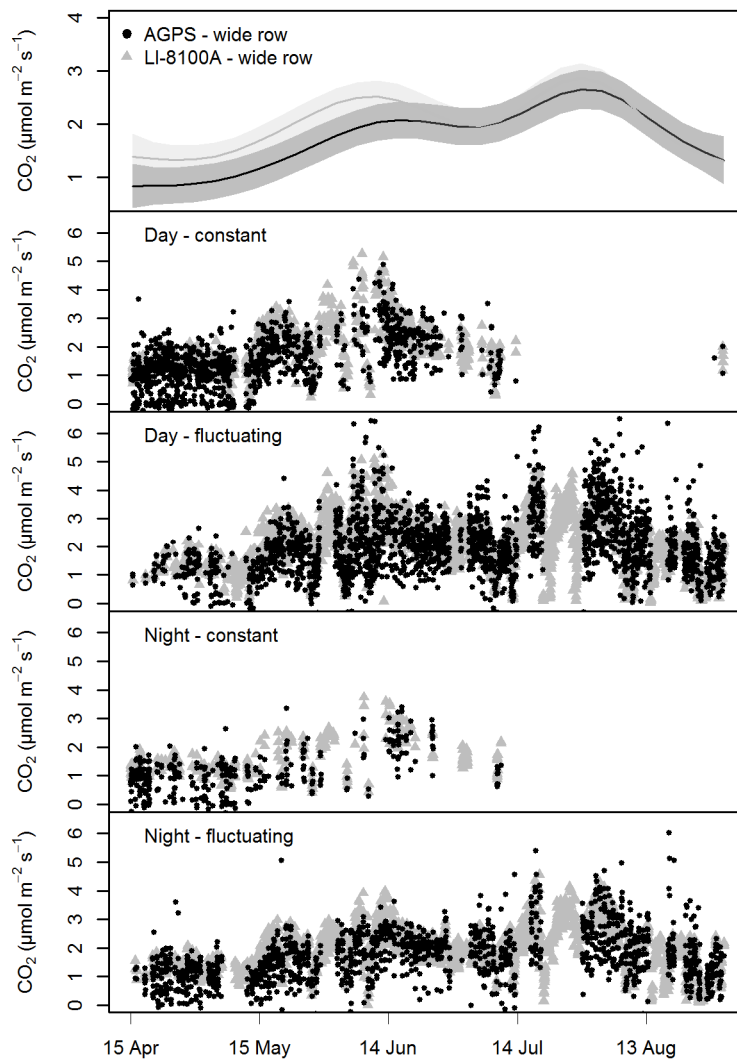
2 Figure 3. Air temperature change inside the chambers during the closure time. For the AGPS,  
 3 temperature change is shown for the first 4 min of the closure time and for 9 min closure time.

4 The LI-8100A had a closure time of 3 min.

5

6



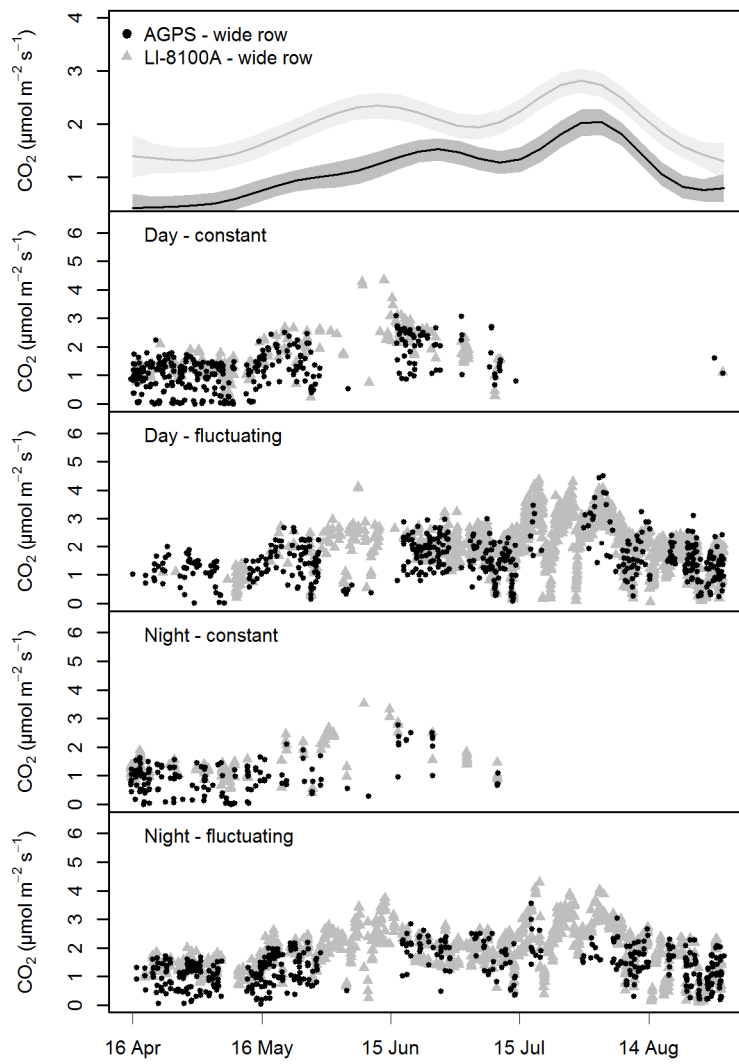


1

2 Figure 4. Unfiltered chamber CO<sub>2</sub> flux datasets for the entire monitoring period (wide rows  
 3 only). The top panel shows the average daily CO<sub>2</sub> flux and its respective 95 % confidence  
 4 interval for each chamber system estimated using generalized additive models (GAM)  
 5 (deviance explained: AGPS 64.9 % (n=896), LI-8100A 58.6 % (n=527)). In the other panels,  
 6 the single measured CO<sub>2</sub> fluxes over time were grouped by time of the day and stability of the  
 7 atmospheric CO<sub>2</sub> concentration at 50 cm above the soil surface. The datasets were divided into  
 8 day and night based on sun rise and sunset times. Atmospheric CO<sub>2</sub> concentration was  
 9 considered as constant when the standard deviation for a 3-min measurement prior to the  
 10 chamber closures was  $\leq 1.0$  ppm. The AGPS CO<sub>2</sub> fluxes were calculated from the first 4 min  
 11 of the closure time (including 1-min deadband).

12

13

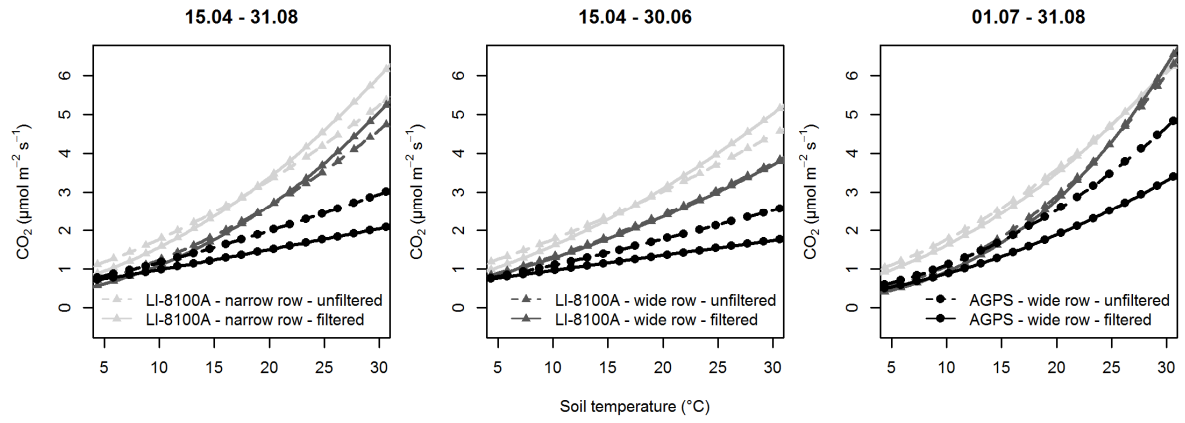


1

2 Figure 5. Filtered chamber CO<sub>2</sub> flux datasets for the entire monitoring period (wide rows only).  
 3 Modelling and grouping of the data is the same as in Fig. 4 (deviance explained for the GAM:  
 4 AGPS 71.1 % (n=582), LI-8100A 57.0 % (n=526)).

5

6

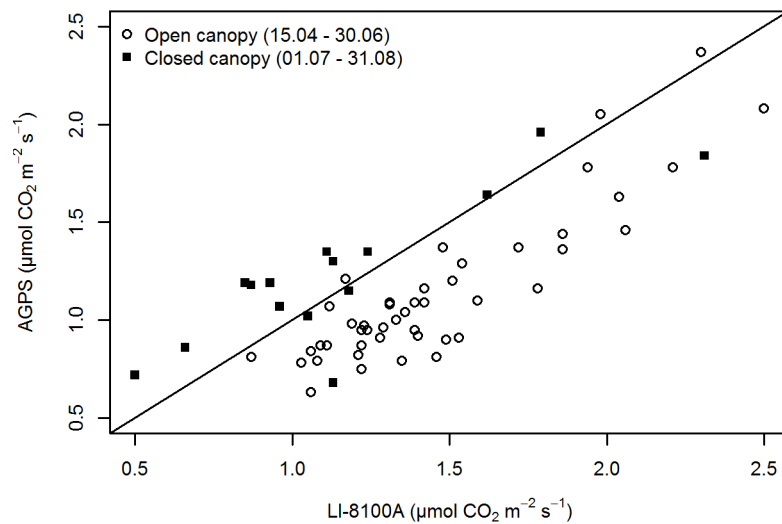


1

2 Figure 6: The Lloyd and Taylor model fitted with the different CO<sub>2</sub> flux datasets for the entire  
 3 monitoring period (15.04 – 31.08.2014), and separately for the open and closed canopy phase  
 4 (15.04 – 30.06.2014 and 01.07 – 31.08.2014, respectively) using soil temperature at 5 cm depth.

5

6



1  
 2 Figure 7. Direct comparison of average CO<sub>2</sub> fluxes obtained with the automated chamber  
 3 systems LI-8100A and AGPS. AGPS fluxes were averaged for each complete measurement  
 4 cycle which consisted of eight chambers run in sequence within a 4 hour window. Only those  
 5 4 hour windows were included in the figure where at least five of the eight chambers passed the  
 6 quality control protocol. Filtered LI-8100A fluxes were averaged for the matching 4 hour  
 7 windows (n=4-8). Standards errors varied between 0.08 and 0.37  $\mu\text{mol CO}_2 \text{ m}^{-2} \text{ s}^{-1}$  for the  
 8 AGPS, and between 0.03 and 0.34  $\mu\text{mol CO}_2 \text{ m}^{-2} \text{ s}^{-1}$  for the LI-8100A, respectively.